

**DEVELOPMENT AND EVALUATION OF
MINIATURE STIRLING ENGINE INTEGRATED
WITH A DC GENERATOR FOR CHARGING
MOBILE DEVICES**

Darren Liu Chon Yon

UNIVERSITI TUNKU ABDUL RAHMAN

**DEVELOPMENT AND EVALUATION OF MINIATURE STIRLING
ENGINE INTEGRATED WITH A DC GENERATOR FOR CHARGING
MOBILE DEVICES**

Darren Liu Chon Yon

**A project report submitted in partial fulfillment of the
requirements for the award of Bachelor of Electrical and Electronic
Engineering with Honours**


**Lee Kong Chian Faculty of Engineering and Science
Universiti Tunku Abdul Rahman**

April 2024

DECLARATION

I hereby declare that this project report is based on my original work except for citations and quotations which have been duly acknowledged. I also declare that it has not been previously and concurrently submitted for any other degree or award at UTAR or other institutions.

Signature :

A handwritten signature in black ink, appearing to read 'Darren Liu Chon Yon', is written over a horizontal line. The signature is stylized and enclosed within a large, loopy oval shape.

Name : Darren Liu Chon Yon

ID No. : 2000980

Date : 24/4/2024

APPROVAL FOR SUBMISSION

I certify that this project report entitled **“DEVELOPMENT AND EVALUATION OF MINIATURE STIRLING ENGINE INTEGRATED WITH A DC GENERATOR FOR CHARGING MOBILE DEVICES”** was prepared by **DARREN LIU CHON YON** has met the required standard for submission in partial fulfilment of the requirements for the award of Bachelor of Electrical and Electronic Engineering with Honours at Universiti Tunku Abdul Rahman.

Approved by,

Signature :



Supervisor :

Prof Lim Yun Seng

Date :

16th May 2024

Signature :

Co-Supervisor :

Date :

The copyright of this report belongs to the author under the terms of the copyright Act 1987 as qualified by Intellectual Property Policy of Universiti Tunku Abdul Rahman. Due acknowledgement shall always be made of the use of any material contained in, or derived from, this report.

© 2024, Darren Liu Chon Yon. All right reserved.

ACKNOWLEDGEMENTS

I would like to thank everyone who contributed to the successful completion of this project. I would like to express my gratitude to my research supervisor, Ir.Prof.Dr.Lim Yun Seng for his invaluable advice, guidance, and enormous patience throughout the development of the research. Furthermore, I am immensely thankful to my family for their unwavering support and encouragement throughout this endeavor. Their constant belief in my abilities and encouragement have been a source of strength and motivation, inspiring me to persevere even in the face of challenges.

In conclusion, I am deeply grateful to all those who have contributed in various capacities, directly or indirectly, towards the completion of this project. Your support and guidance have been invaluable, and I am truly humbled by your generosity and dedication.

ABSTRACT

Utilization of Stirling engines is the main focus of this study for portable power generation, offering a versatile solution for areas lacking access to power grids. The Stirling engine's ability to harness various heat sources, including solar energy and biomass, presents a promising avenue for sustainable energy production. However, despite theoretical predictions suggesting high efficiency comparable to the Carnot cycle, practical implementations exhibit constrained thermal efficiency, posing a significant challenge for electricity generation applications. This study aims to address this discrepancy by identifying and recommending viable solutions to enhance the efficiency and power output of small-scale Stirling engines. By bridging the gap between theory and practice, this research seeks to unlock the full potential of Stirling engines as reliable and efficient energy solutions, contributing to sustainable development and energy access in underserved regions. The results presented offer a comprehensive comparison of Stirling engine output power across various configurations. Notably, the analysis reveals the superior performance of a Stirling engine equipped with a larger diameter titanium displacer and a 100° phase angle, underscoring the importance of optimization in maximizing power output. Overall, this study contributes to a deeper understanding of Stirling engine dynamics and provides insights into strategies for improving efficiency and performance. By addressing key challenges and offering practical solutions, the study paves the way for the broader adoption of Stirling engines as integral components of sustainable energy systems.

TABLE OF CONTENTS

DECLARATION		i
APPROVAL FOR SUBMISSION		ii
ACKNOWLEDGEMENTS		iv
ABSTRACT		v
TABLE OF CONTENTS		vi
LIST OF TABLES		ix
LIST OF FIGURES		x
LIST OF SYMBOLS / ABBREVIATIONS		xiii
CHAPTER		
1	INTRODUCTION	1
1.1	General Introduction	1
1.2	Importance of the Study	2
1.3	Problem Statement	3
1.4	Aim and Objectives	4
1.5	Contribution of Study	4
1.6	Scope and Limitation of the Study	5
1.7	Outline of the Report	6
1.8	Project Management	7
2	LITERATURE REVIEW	8
2.1	Introduction	8
2.2	Concept of Stirling engine integrated with a DC generator	8
2.3	Main Parts and Working Principles of Stirling Engine	10
2.4	Types of Stirling Engine	11
2.5	Performance Comparison of Different Types of Stirling Engines	13

2.6	Phase Angle Effects on Stirling Engine's Performance	16
2.7	Dead Space Effects on Stirling Engine's Performance	19
2.8	Matrix Conductivity and Heat Capacity of the Regenerator Effects on Stirling Engine's Performance	21
2.9	Summaries Existing Studies from Review	22
2.10	Related Projects	23
	2.10.1 Electricity Production In Rural Villages With A Biomass Stirling Engine	23
	2.10.2 The Application Of An Innovative Integrated Swiss-roll-combustor On A Stirling Engine	24
	2.10.3 Review On Solar Stirling Engine: Development and Performance	25
2.11	Summary	27
3	METHODOLOGY AND WORK PLAN	28
3.1	Introduction	28
	3.1.1 Development Methodology	29
3.2	Process Flowchart	30
3.3	Engine Manufacturing	31
3.4	System Setup	33
	3.4.1 Electrical Connection of the Charging System	36
3.5	Tools	37
	3.5.1 RF-370 DC Motor Generator	37
	3.5.2 Online Pulley Simulation	38
	3.5.3 Stirling Engine Speed Regulator	39
	3.5.4 DC-DC Boost Converter	40
	3.5.5 12V DC Brushless Cooling Fan	43
	3.5.6 Liquid Cooling Radiator	44
	3.5.7 12V DC Pneumatic Diaphragm Water Pump	45

	3.5.8 12V DC Power Supply	46
	3.5.9 SolidWorks	47
	3.6 Summary	48
4	RESULTS AND DISCUSSION	49
	4.1 Introduction	49
	4.2 Measuring System	50
	4.3 Output Power of the System	51
	4.3.1 Aluminium Displacer with Diameter of 39mm (90° phase angle)	51
	4.3.2 Titanium Displacer with Diameter of 39mm (90° phase angle)	56
	4.3.3 Titanium Displacer with Diameter of 35mm (90° phase angle)	59
	4.3.4 Titanium Displacer with Diameter of 39mm (100° phase angle)	61
	4.4 Highest Achievable Output Power	63
	4.5 Charging Circuit Design	64
	4.6 Summary	66
5	CONCLUSIONS AND RECOMMENDATIONS	67
	5.1 Conclusions	67
	5.2 Problems Encountered	68
	5.3 Recommendations for Future Enhancement	69
	REFERENCES	70

LIST OF TABLES

Table 2.1:	Evaluation of the performance attributes of the three Stirling engine variations (α , β , and γ)(Abuelyamen and Ben-Mansour, 2018)	13
Table 2.2:	Effect of the regenerator material on engine performance.(Timoumi et al., 2008)	21
Table 2.3:	Summary of Existing Studies	22
Table 2.4:	Test Results of Biomass Stirling Engine (Podesser, 1999)	23
Table 3.1:	Features of RF-370 DC Motor Generator	37
Table 3.2:	Features of DC-DC Boost Converter	41
Table 3.3:	Features of HT7750/ SOT23 Converter	41

LIST OF FIGURES

Figure 1.1:	Gantt Chart	7
Figure 2.1:	Gamma Stirling engine (Steinhardt, 2015)	8
Figure 2.2:	Concept of Stirling Engine integrated with DC generator	8
Figure 2.3:	Main parts of Stirling engine.(Anon, n.d.)	10
Figure 2.4:	Schematic diagram of different types of Stirling engines. (Alfarawi, et al., 2016)	12
Figure 2.5:	Temperature distributions at various crank angles for a Stirling engine of the β -type. (Abuelyamen and Ben- Mansour, 2018)	14
Figure 2.6:	Temperature distributions at various crank angles for a Stirling engine of the γ -type. (Abuelyamen and Ben- Mansour, 2018)	14
Figure 2.7:	Influence of phase angle on engine performance, (a) shaft power, and (b) engine efficiency. (Senft, 2002)	16
Figure 2.8:	Pressure reduction across the regenerator in relation to the crank angle at varying phase angles. (Alfarawi, Al- Dadah, et al., 2016)	17
Figure 2.9:	Pressure vs volume at different phase angles. (Alfarawi, AL-Dadah, et al., 2016)	18
Figure 2.10:	Influence of connecting pipe diameter on engine power performance. (Alfarawi, AL-Dadah, et al., 2016)	20
Figure 2.11:	Swiss-roll-combustor Stirling Engine (Wu et al., 2021)	24
Figure 2.12:	Swiss-roll-combustor (Wu et al., 2021)	24
Figure 2.13:	Dish-Stirling engine with different components (Singh and Kumar, 2018)	25
Figure 3.1:	Product development life cycle	29
Figure 3.2:	Process Flowchart	30
Figure 3.3:	Bend saw to cut the metal bar	31
Figure 3.4:	Lathe machine to obtain the required diameter of the metal cylinder	32

Figure 3.5:	Setup of Stirling engine prime-mover	33
Figure 3.6:	Flywheel of Stirling engine	34
Figure 3.7:	3D-printed coupling pulley-set	34
Figure 3.8:	Cooling system components	35
Figure 3.9:	Cooling system attached to the Stirling engine	35
Figure 3.10:	Connection of charging system	36
Figure 3.11:	DC motor RF-370	37
Figure 3.12:	Pulley simulation	38
Figure 3.13:	Speed Regulator	39
Figure 3.14:	DC-DC Boost Converter	40
Figure 3.15:	Circuit of DC-DC boost converter	41
Figure 3.16:	HT7750/ SOT23	42
Figure 3.17:	Pin Configuration of converter HT7750/ SOT23	42
Figure 3.18:	12V DC Brushless Cooling Fan	43
Figure 3.19:	Liquid Cooling Radiator	44
Figure 3.20:	12V DC Pneumatic Diaphragm Water Pump	45
Figure 3.21:	12V DC Power Supply	46
Figure 3.22:	Pulley Designed	47
Figure 3.23:	Logo of SolidWorks	47
Figure 4.1:	Measurement system	50
Figure 4.2:	Graph of current against voltage across the variable resistor	52
Figure 4.3:	Graph of DC generator's power against voltage across variable resistor	53
Figure 4.4:	Graph of speed Stirling engine's flywheel against voltage across variable resistor	54
Figure 4.5:	Graph of current against voltage	56

Figure 4.6:	Graph of DC generator's power against voltage	57
Figure 4.7:	Graph of speed Stirling engine's flywheel against voltage across variable resistor	58
Figure 4.8:	Graph of current against voltage	59
Figure 4.9:	Graph of DC generator's power against voltage	60
Figure 4.10:	Graph of current against voltage	61
Figure 4.11:	Graph of DC generator's power against voltage	62
Figure 4.12:	Highest Achievable Output Power of Different Model Stirling Engine	64
Figure 4.13:	Charging circuit board	64
Figure 4.14:	System charging indications	65

LIST OF SYMBOLS / ABBREVIATIONS

DC	direct current
TH	temperature hot
TC	temperature cold

CHAPTER 1

INTRODUCTION

1.1 General Introduction

The development of advanced technologies that serve to provide energy is one of the problems that people are attempting to solve today, from the use of fire to natural resources such as fossil fuel and coal to generate electricity with engines. Since the beginning of time, as we know it, the world has been propelled by engines. Start-up and running of engines or generators require natural resources such as fossil fuels in order to generate electricity. The majority of our daily activities, such as phone recharge and illumination, are dependent on the supply of electricity. However, there are circumstances in which petrol generators or supply of electricity may not be available (Shufat et al., 2019). Therefore a mobile generating unit that is able to generate electricity for portable devices will be very useful. It is hence proposed a project to develop a generating unit using a Stirling engine coupled with the DC generator. The Stirling engine will run depending on the heat source which can be either from the wood fire or solar heat (Ahmadi et al., 2013).

Using a Stirling engine to generate electricity is an additional convenient way of providing electricity for portable devices. The Stirling engine can be launched in the wild by burning firewood, butane, and wooden objects to generate heat. Using this method, a sufficient quantity of electricity can be generated regardless of whether it is daytime or nighttime or whether there is sufficient sunlight. Moreover, a Stirling engine generator could be useful in the event of a natural disaster. For instance, when an earthquake causes power disruptions or an abrupt blackout, the Stirling engine can be used as a temporary power source for lighting and other low-voltage devices. A Stirling engine is a heat engine that operates through the cyclical compression and expansion of air between varying temperature levels, which results in the net conversion of heat energy to mechanical labor. The Stirling engine is then combined with a direct current (DC) generator to produce electricity for charging mobile devices and powering small devices.

1.2 Importance of the Study

The study of the Stirling engine is important for advancing and enabling remote power generation, where the production of electricity in areas that are geographically isolated or have limited access to traditional power grids. These areas can include rural communities, off-grid locations, and even mobile or temporary installations. Stirling engines have been recognized as a viable technology for remote power generation due to their versatility and fuel flexibility. Fuel flexibility means that Stirling engines can operate with a wide range of fuels, making them suitable for remote or off-grid applications. Studying Stirling engines can help in optimizing their performance and adapting them to specific remote power generation needs, improving access to energy in underserved regions.

Besides butane and wooden objects, Stirling engines can also be used with a variety of heat sources, including solar energy, biomass, and waste heat. Understanding the principles and operation of Stirling engines enables the development of energy systems that harness these heat sources efficiently. This study would also contribute to the advancement of sustainable and environmentally friendly energy solutions.

1.3 Problem Statement

Based on the operating principle, The Stirling engine's optimal cycle exhibits a thermal efficiency that is equivalent to that of a Carnot cycle. A Carnot cycle is an ideal thermodynamic cycle that has a very high efficiency. In a Carnot cycle, the Stirling engine transfers energy in the form of heat between two thermal reservoirs at two extreme temperatures, namely T_H and T_C . Given that T_H is referred to as the hot reservoir, and T_C is referred to as the cold reservoir. Part of this transferred energy is converted to the work done by the Stirling engines. However, in actual real situations, the Stirling engine prototype shows only a small thermal efficiency.

The main issue at hand pertains to the constrained thermal efficiency observed in small-scale Stirling engines. The ultimate objective is to augment both their efficiency and power output, particularly for the purpose of electricity generation. This becomes especially crucial as the stability of the voltage generated holds significant importance for the Stirling engine to function effectively as a portable charging device.

Moreover, there are a few limitations of current charging solution methods. For example, most of the electrical sources rely on grid electricity or have limited battery capacity. Secondly, there is a lack of awareness, many people are more familiar with solar panels and wind turbines as sustainable energy sources which leads to very little relevant research being done as compared to other sustainable energy, despite Stirling engines having been around for a long time.

The aim of this study is to identify and recommend viable solutions to address the aforementioned issue, ultimately working towards achieving the desired result.

1.4 Aim and Objectives

There are three objectives in this project:

1. To fabricate the Stirling engine as a prime mover.
2. To evaluate the performance of the Stirling engine when connected to load.
3. To improve the efficiency and performance of the Stirling engine.

1.5 Contribution of Study

This study makes a substantial contribution to the field of sustainable energy generation through its innovative approach to integrating a miniature Stirling engine with a DC generator for charging mobile devices. By successfully developing and evaluating this integrated system, the project not only demonstrates the feasibility of utilizing Stirling engine technology in practical applications but also provides valuable insights into its performance and efficiency. This contribution extends beyond theoretical research, offering a tangible solution to modern energy needs in scenarios where conventional power sources may be limited or unavailable. Furthermore, the project's findings pave the way for future advancements in Stirling engine technology and its integration into portable power generation solutions, thus advancing the pursuit of sustainable energy solutions for a variety of real-world applications.

1.6 Scope and Limitation of the Study

This study does have certain limitations that need to be considered. These limitations encompass aspects like heat source compatibility, scaling, and size restrictions, as well as external factors.

To delve deeper, it's important to note that the performance and efficiency of Stirling engines are profoundly influenced by the characteristics and accessibility of the heat source. Various heat sources may impose restrictions or challenges when paired with Stirling engines. As a result, it is crucial for the study to thoroughly assess and weigh the compatibility and feasibility of different heat sources, particularly in relation to their suitability for specific applications.

Next, scaling Stirling engines to different power levels can pose challenges in terms of mechanical design, heat transfer, and system integration. The study should address the scaling issues and assess the size constraints and limitations associated with the desired power output and application requirements.

Besides that, the performance of the Stirling engines can also be influenced by various external factors, such as ambient temperature, humidity, altitude, or fuel quality. These factors may introduce inaccuracy or variations in the study's results. The research needs to be carried out and controlled carefully in order to minimize inaccuracy and to ensure the reliability of the studies.

1.7 Outline of the Report

Chapter 1 Introduction discourses the general introduction, importance of the study, problem statement, aim and objectives, contribution of study, and scope and limitation of the study.

Chapter 2 Literature Review evaluates the performance of various Stirling engine types, analyzing factors such as the phase angle between the displacer piston and work piston, cylinder dead space volume, and material composition of the displacer piston. Additionally, this chapter incorporates relevant research findings from professional papers, studies, and journals.

Chapter 3 Methodology explains the proposed project's work plan methodology. It also delineates the necessary hardware and software components, along with integration techniques for both the charging and cooling systems.

Chapter 4 Result and Discussion discusses the results collected from the measurement process, particularly focusing on the output power of the DC generator coupled with the Stirling engine. Different Stirling engine models are compared based on experimental data.

Chapter 5 Conclusion and Recommendations concludes the project findings with an analysis and discussion of the results obtained. The conclusion of this study is made according to the objective to be achieved and the results obtained. Recommendations for the future enhancement are also being discussed in this chapter.

1.8 Project Management

Figure 1.1 shows the Gantt chart created for this project. The project is to be completed within two trimesters.

Task	First Trimester (Weeks)														Second Trimester (Weeks)													
	1	2	3	4	5	6	7	8	9	10	11	12	13	14	1	2	3	4	5	6	7	8	9	10	11	12	13	14
Understanding the objectives and problems	█	█																										
Project Research		█	█																									
Hands-on overhauling prototype		█	█	█	█																							
Project Research					█	█	█																					
Materials purchase							█	█																				
Interim report writing							█	█	█	█	█																	
Interim report presentation & submission										█	█	█	█	█														
Do amendments on report															█	█												
Materials installation for testing																█	█	█										
Data collection																		█	█	█	█							
Report writing																					█	█	█					
Finalized report writing & Hardware																						█	█	█	█			
Poster design																									█	█	█	
Report presentation & submission																											█	█

Figure 1.1: Gantt Chart

CHAPTER 2

LITERATURE REVIEW

2.1 Introduction

This chapter describes the integration of a Stirling engine with a direct current (DC) generator as a solution to the power scarcity problem encountered when charging mobile devices. The system's concept will also be presented in this section. In addition, the Stirling engine's working principle and the performance of numerous types of Stirling engines will be reviewed. Moreover, factors that affect the performance of the Stirling engine will also be reviewed. Conference papers and journals are the primary sources to be reviewed.

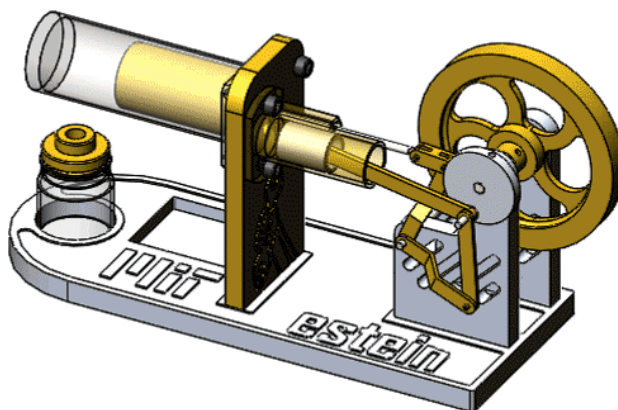


Figure 2.1: Gamma Stirling engine (Steinhardt, 2015)

2.2 Concept of Stirling engine integrated with a DC generator

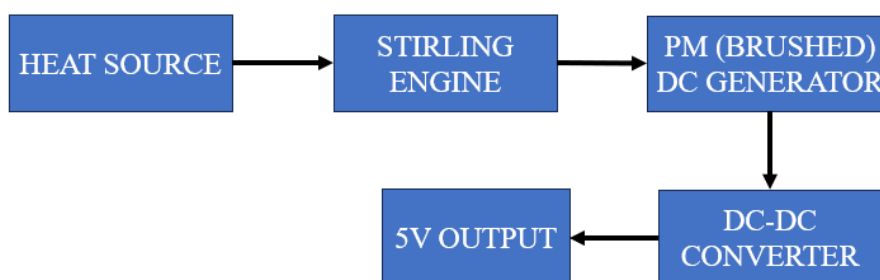


Figure 2.2: Concept of Stirling Engine integrated with DC generator

The heat source functions as the primary energy input for the entire system, generating the necessary temperature difference for the Stirling engine to operate. It is not limited to a specific variety and will be powered by Ethanol. Consequently, the heat source's output serves as the input for the Stirling engine, facilitating its operation.

The Stirling engine functions as the primary mechanical device in the system. By harnessing the temperature disparity between the hot and cold sections within the operational gas chamber, a cyclic procedure is initiated, consisting of four fundamental phases: cooling, compression, heating, and expansion. As a result, the Stirling engine efficiently converts the thermal energy provided by the heat source into mechanical energy. The Stirling engine's output shaft will then be connected to the DC generator's rotor. The DC generator is tasked with the conversion of mechanical work, generated by the Stirling engine, into electrical energy. The direct current (DC) generator will produce an output in the form of a direct current generated by the stator windings. This direct current will then be utilized as the input for the DC-DC boost converter.

In addition, the DC-DC boost converter functions as the voltage regulator for the system and will be carefully engineered to fulfill the specific performance requirements of the system. The major purpose of this device is to work as a direct current (DC) transformer, producing a consistent and purified DC signal with an estimated voltage of 5V. Moreover, the DC-DC converter is capable of efficiently regulating the output voltage to a constant value of 5V, even in the presence of input voltage fluctuations caused by changes in the speed of the Stirling engine. As a result, the consistent 5V direct current (DC) output generated by the converter will function as a reliable power supply for the purpose of charging mobile devices.

2.3 Main Parts and Working Principles of Stirling Engine

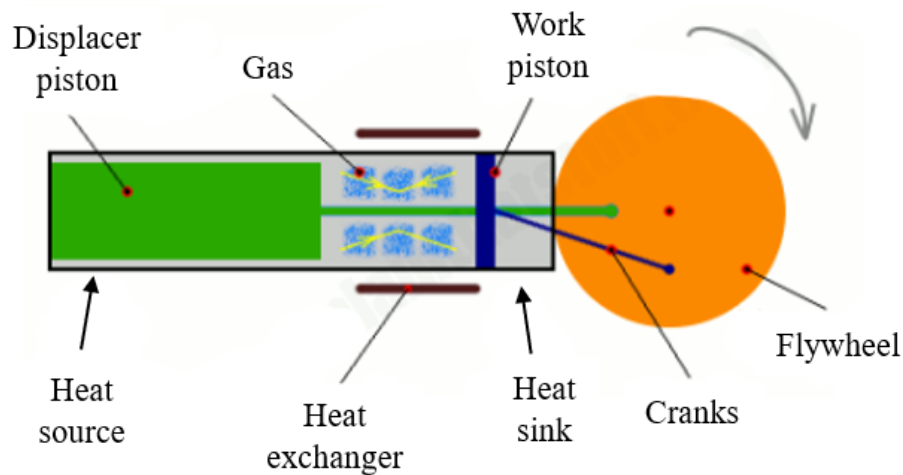


Figure 2.3: Main parts of Stirling engine.(Anon, n.d.)

The primary components of the Stirling engine include the displacer piston, work piston, heat sink, crankshaft, and flywheel.

The apparatus comprises a constant quantity of gas confined within a sealed cylinder. The gas utilized in this context, which may consist of common air, hydrogen, helium, or any other easily obtainable substance that remains in its gaseous form during the whole heating and cooling cycle of the engine, fulfills a distinct purpose. The major function of this system is to facilitate the flow of thermal energy from the heat source to the heat sink, thereby powering the piston responsible for driving the machine's operation. Subsequently, the system repeats this procedure. The heat sink functions as the site where the heated gas undergoes cooling prior to its reintegration with the heat source. The function of the object is comparable to that of a radiator, as it dissipates excess heat into the surrounding atmosphere. In comparison to a traditional piston used in a steam engine, the displacer in this system is intentionally designed to have an adequate tolerance, leading to a minimal gap between the outer edge of the displacer and the inner surface of the cylinder. Consequently, the gaseous substance circulates along the outside edge of the displacer during its oscillatory motion. Moreover, an appropriately sealed and closely fitted working piston is situated inside the cylindrical chamber, effectively transforming the expansion of the gas into useful mechanical energy that

drives the machinery propelled by the engine. In order to facilitate efficient functioning, a flywheel is affixed to the system, therefore accumulating rotational inertia. Both the work piston and the displacer exhibit perpetual motion; nevertheless, their motions are characterized by a phase difference of 90 degrees. Both the displacer piston and the working piston are driven by the same wheel, however, the displacer piston consistently maintains a one-quarter cycle lead over the working piston. The heat exchanger, commonly known as the regenerator, is strategically located within the enclosed chamber, situated between the heat source and the heat sink. As the gaseous medium traverses the regenerator, it liberates a fraction of its thermal energy, afterward being absorbed and conserved by the regenerator. Upon the return of the gas, it undergoes the process of reabsorbing the heat that was previously stored. The inclusion of the regenerator is of utmost importance as it serves to limit the dispersion of this important thermal energy into the surrounding atmosphere, thus mitigating any potential loss. The incorporation of a heat exchanger, commonly referred to as a regenerator, yields a significant enhancement in both the efficiency and power generation of the engine. (Woodford, et al., 2023).

2.4 Types of Stirling Engine

The mechanical arrangement of conventional Stirling engines can be categorized into three distinct configurations, specifically α , β , and γ , as seen in Figure 2.4. Other types include thermoacoustic (Backhaus and Swift, 1999), Ringbom (Senft, 1993), and fluid Stirling engine (Elrod, 1974). The α -type Stirling engine configuration involves the placement of separate cylinders for the hot and cold work pistons, which are positioned on opposite sides of the regenerator. The installation of this specific engine layout often involves the usage of the V arrangement and the yoke drive, commonly referred to as the Ross linkage (Alfarawi, Al-Dadah, et al., 2016).

Moreover, a β -type Stirling engine is comprised of a working piston and a displacer piston that are integrated within a single cylinder. However, it is important to note that a significant mechanical limitation arises from the existence of a driving rod that extends through the working piston, originating from the displacer piston. On the other hand, the use of less dead space has the

potential to result in improved compression, efficiency, and power (Alfarawi, Al-Dadah, et al., 2016). The term "dead volume" in the context of a Stirling engine pertains to the volume encompassed by the engine's cylinders and passages that do not actively participate in the power generation process. The working fluid's spatial occupancy during various phases of the engine's operation is denoted by this term, but it does not actively contribute to the engine's overall performance. The utilization of the rhombic driving mechanism is frequently observed in this particular sort of engine.

Furthermore, it is essential to acknowledge that within a γ -type Stirling engine, the working piston and the displacer piston are situated within distinct cylinders. The piston, located on the cooler side of the cylinder, undergoes expansion and compression as it facilitates the intake of gas into the cylinder. The current engine configuration has a higher level of mechanical efficiency in comparison to other configurations. However, The system exhibits large dead volumes when compared to other types of Stirling engines, namely in the connecting pipe that links the compression area to the bottom section of the expansion space. The usage of the conventional crank drive is commonly employed in engines of this type (Alfarawi, Al-Dadah, et al., 2016).

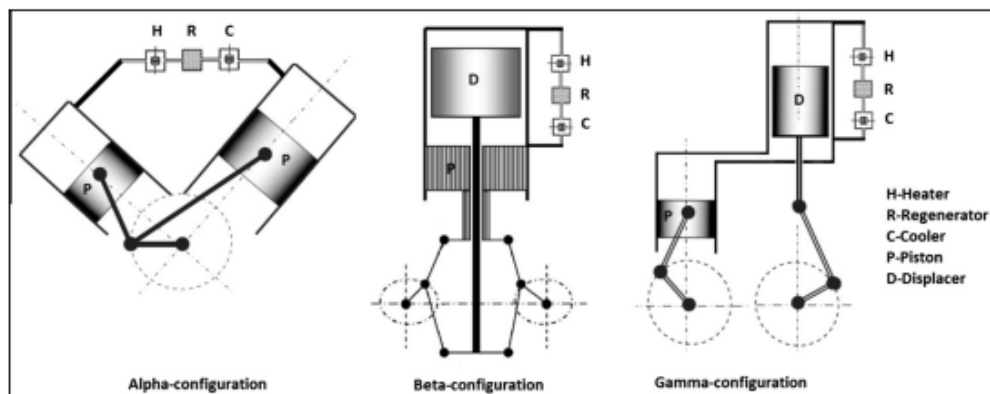


Figure 2.4: Schematic diagram of different types of Stirling engines. (Alfarawi, et al., 2016)

2.5 Performance Comparison of Different Types of Stirling Engines

The research undertaken by Ahmed Abuelyamen and Rached Ben-Mansour presents a comprehensive analysis of performance comparisons among several types of Stirling engines using the detailed computational fluid dynamics (CFD) modeling technique. According to the results obtained from the computational fluid dynamics (CFD) algorithm, the α -type Stirling engine demonstrates the lowest power output and thermal efficiency, with measurements of 0.9 W and 1.8%, respectively. Subsequently, a β -type Stirling engine was employed, revealing a slightly greater power output and thermal efficiency in comparison to the α -type Stirling engine, with values of 8.7 W and 7.5%, respectively. γ -type Stirling engines have been observed to achieve the highest recorded power output and thermal efficiency, measuring 9.22 W and 9.8%, respectively (Abuelyamen and Ben-Mansour, 2018).

Table 2.1: Evaluation of the performance attributes of the three Stirling engine variations (α , β , and γ)(Abuelyamen and Ben-Mansour, 2018)

Performance of the three Stirling engine types (α , β and γ).					
	Q_{in} (W)	Q_{out} (W)	Q_{net} (W)	W_{out} (W) = $\int PdV$	Efficiency
α -type	50.5	-47.4	3.119	0.908	1.8%
β -type	115.9	-107.1	8.704	8.634	7.5%
γ -type	94.2	-83.9	10.256	9.223	9.8%

The investigation has revealed that the reduced efficiency of the α -type Stirling engine can be attributed to its restricted capacity to absorb heat. As indicated in Table 2.1, it becomes evident that the α -type Stirling engine absorbs 50.5W of heat, which is approximately half of the heat absorbed by the β -type Stirling engine, totaling 115.9W. Conversely, the γ -type Stirling engine absorbs 21.7W less heat compared to the β -type Stirling engine. Nevertheless, the γ -type Stirling engine maintains a higher power output in comparison to the β -type Stirling engine (Abuelyamen and Ben-Mansour, 2018).

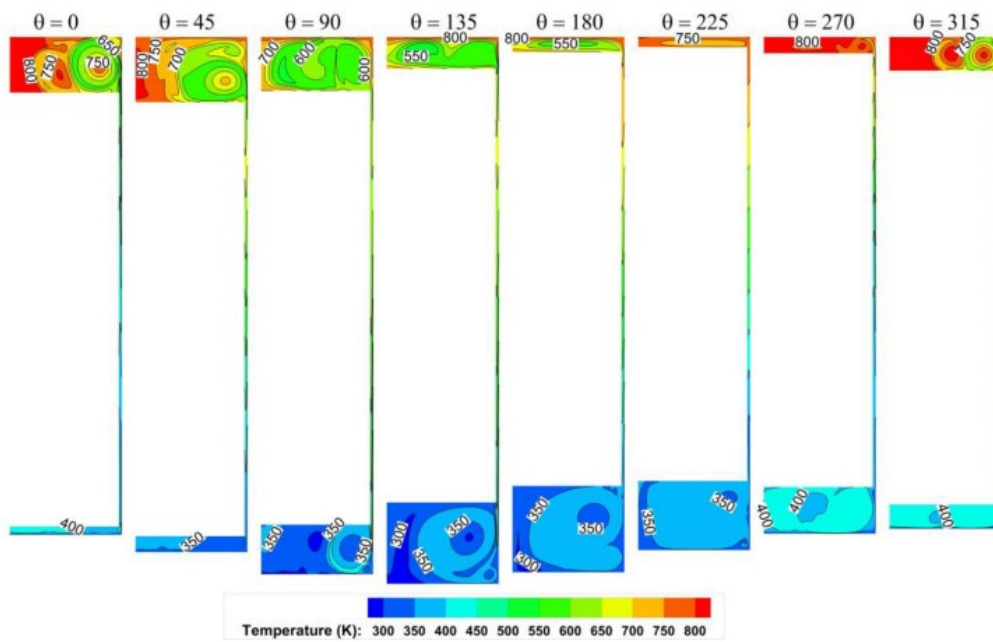


Figure 2.5: Temperature distributions at various crank angles for a Stirling engine of the β -type. (Abuelyamen and Ben-Mansour, 2018)

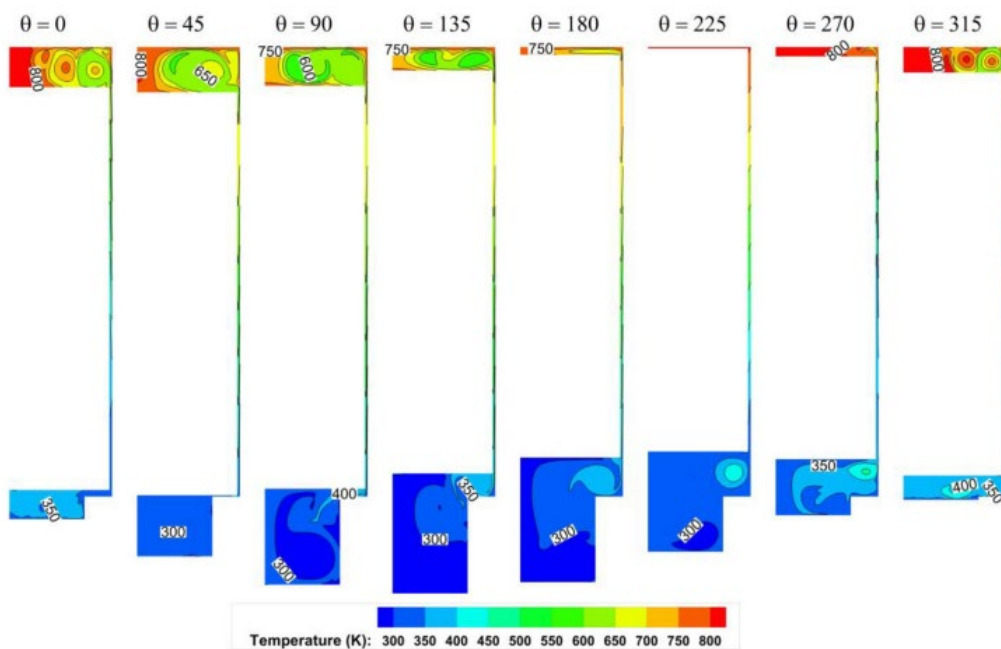


Figure 2.6: Temperature distributions at various crank angles for a Stirling engine of the γ -type. (Abuelyamen and Ben-Mansour, 2018)

To further clarify the rationale for the higher efficiency exhibited by the γ -type Stirling engine in comparison to the β -type Stirling engine, Figure 2.5 and Figure 2.6 depict the temperature contours of both engine types. The temperature patterns observed in both the hot zone and the narrow channel exhibit a significant level of similarities in the two types mentioned above. However, it's important to point out that the γ -type Stirling engine shows a relatively lower temperature in the cold zone compared to the temperature observed in the β -type Stirling engine. The Stirling engine of the γ configuration facilitates the generation of many vortices throughout the whole cold zone as a consequence of the reduction in pipe size and the movement of the piston. This phenomenon leads to effective gas mixing. On the contrary, within the cold region of the β -type Stirling engine, a single vortex is generated.

Moreover, as depicted in Figure 2.6, the positioning of the displacer in the initial quarter of the cycle is observed to be in close proximity to the lower section of the large cylinder. Consequently, this arrangement leads to the formation of a supplementary narrow channel between the lower portion of the large cylinder and the bottom of the displacer. As a result, the gases are brought into the cold zone at a somewhat lower temperature, approaching that of the cooler side. During the initial quarter of the cycle, the gas exhibits higher pressure, resulting in the exertion of force on the piston, generating useful work. Simultaneously, the gas undergoes a decrease in temperature upon its entry into the cold zone (Abuelyamen and Ben-Mansour, 2018).

During the subsequent phase of the cycle, denoted as $= 90 - 180$, the displacer facilitates the movement of the heated gas from the high-temperature area to the low-temperature area. The γ -type Stirling engine has the capability to reach a lower temperature level when compared to the β -type Stirling engine. This phenomenon can be attributed to the effective gas mixing observed within the cold zone of the γ -type Stirling engine. When the temperature of the gas is reduced, the compression process requires a relatively low amount of power. It can be inferred that a γ -type Stirling engine uses less power during the compression process than a β -type engine. These are the reasons found out in this study why γ -type Stirling engine has higher efficiency as compared to the β -type Stirling engine although the heat

absorbed by the γ -type Stirling engine is lower than that of the β -type Stirling engine (Abuelyamen and Ben-Mansour, 2018).

2.6 Phase Angle Effects on Stirling Engine's Performance

James R. Senft conducted a study to investigate how the performance of Stirling engines is influenced by changes in the phase angle. In the majority of gamma-type Stirling engines, it is possible to manipulate the phase angle to optimize shaft power output in accordance with the prevailing operating conditions. It is often accepted that the optimal phase angle for practical purposes is typically regarded to be 90° for practical purposes. Nonetheless, in line with the study's discoveries, Figure 2.7 illustrates that the highest shaft power, amounting to 525 W, is achieved at a phase angle of 100° , as opposed to 503 W at a 90° phase angle.

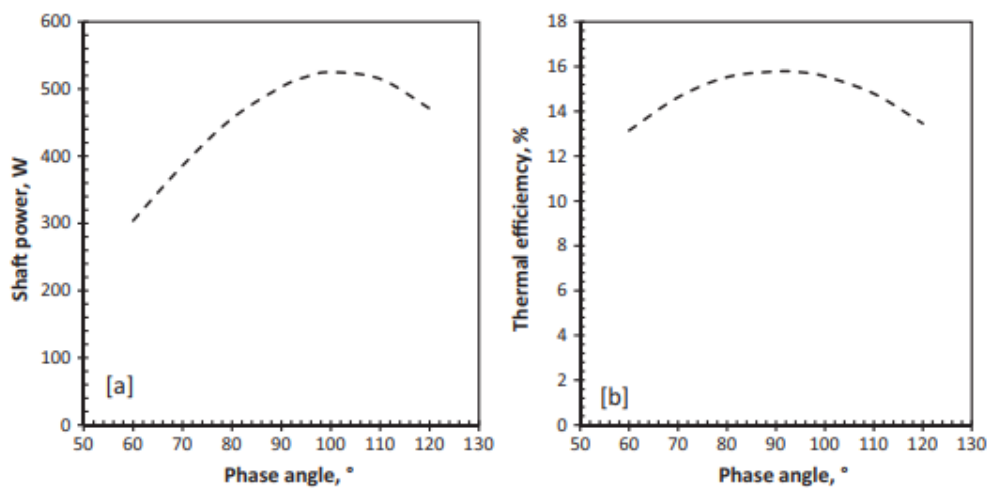


Figure 2.7: Influence of phase angle on engine performance, (a) shaft power, and (b) engine efficiency. (Senft, 2002)

In another study, S. Alfarawai et al. conducted an investigation of the impact of phase angle on the power output of a gamma Stirling engine. The researchers employed computational fluid dynamics (CFD) modeling techniques for their analysis. They found out that variation of phase angle was acknowledged as one of the best ways to control Stirling engine power. The choice of phase angle has significant implications for several aspects, such as pressure amplitude, overall volumetric alteration of the gas, heat transfer, and consequently, the engine's indicated power. The diagram presented in Figure 2.8 depicts the influence of alterations in phase angle on the cyclic pressure variation experienced by the regenerator. In the scenario when the phase angle is set at 90° , the regenerator experiences a maximum pressure decrease of 0.31 bar. While the phase angle was varied from 60° to 120° , an increase in the maximum pressure drop was observed, rising from 0.19 bar to 0.42 bar. Typically, a crank angle shift of approximately 10° is observed where the occurrence of lowest and maximum pressure drop takes place. (Alfarawi, AL-Dadah, et al., 2016).

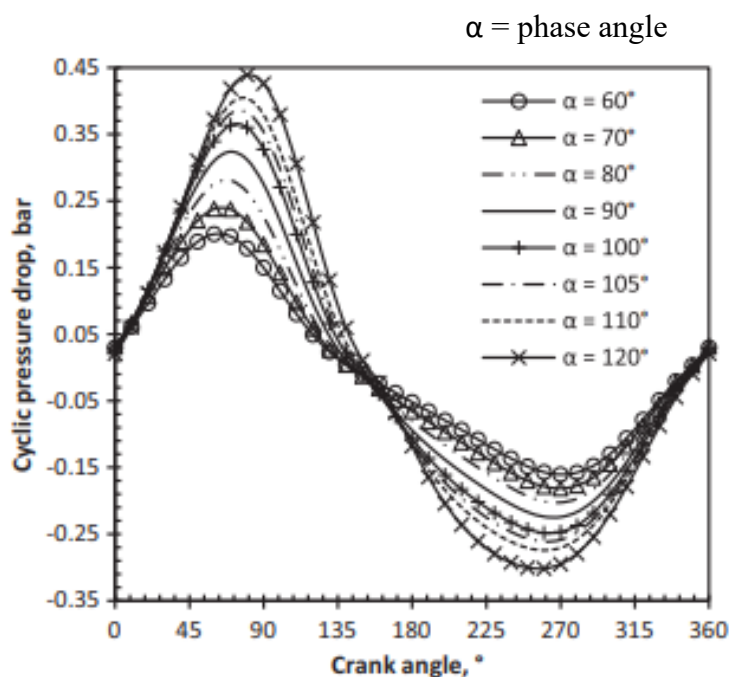


Figure 2.8: Pressure reduction across the regenerator in relation to the crank angle at varying phase angles. (Alfarawi, Al-Dadah, et al., 2016)

Furthermore, Figure 2.9 illustrates how the indicated pressure-volume (PV) diagram is affected by changes in the phase angle. It is noticeable that when the phase angles increase, there is a corresponding increase in the amplitude of the resulting pressure. The relationship between phase angles and pressure amplitude becomes apparent when observing that greater phase angles correspond to increased pressure amplitudes. According to the findings presented in Figure 2.9, it has been observed that the Stirling engine achieves its maximum power output of 750W when operating at a phase angle of 105° (Alfarawi, AL-Dadah, et al., 2016). The phase angle reported in this study is consistent with the results of prior research conducted by James R. Senft, which suggest that the highest shaft power is achieved at a phase angle of 100°, rather than 90°.

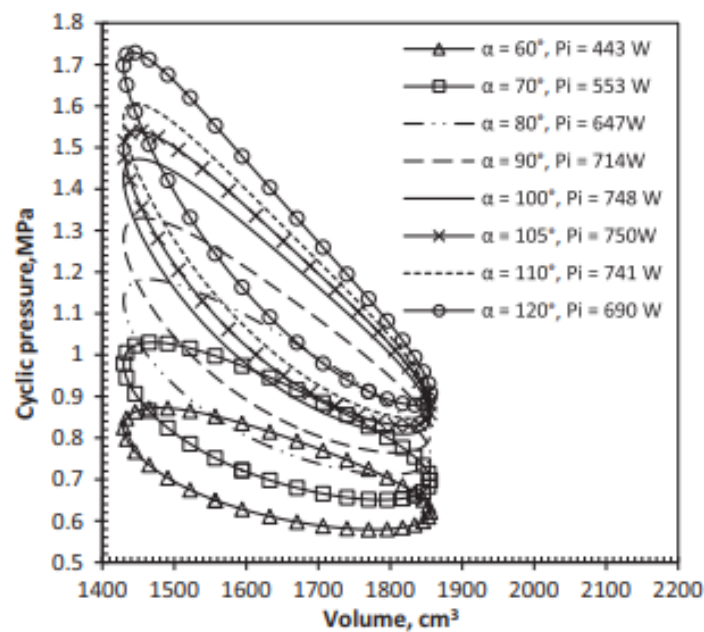


Figure 2.9: Pressure vs volume at different phase angles. (Alfarawi, AL-Dadah, et al., 2016)

2.7 Dead Space Effects on Stirling Engine's Performance

A study was undertaken by Alfarawi et al. to examine the impact of dead space on the operational efficiency of a Stirling engine. The investigation was conducted through the utilization of computational fluid dynamics (CFD) simulation. Based on the CFD simulation, researchers realized that the presence of dead space can have detrimental effects on the performance of the Stirling engine. According to the theoretical framework, it is recommended to minimize the unswept volume. However, this recommendation appears to be in conflict with the practical reality of Stirling engines, as they can possess a dead volume that accounts for as much as 50% of their entire gas volume. After conducting a thorough analysis of the current gamma Stirling engine, observations have revealed that the connecting pipe, which links the compression space to the lower portion of the expansion space, possesses a significantly larger dimension when compared to the dead space volume found in other Stirling engines.

According to the research conducted by S. Alfarawi et al., it is possible to decrease the diameter of the connecting pipe and thus reduce the dead space volume in the Stirling engine without making many modifications to the overall design. This may be achieved by implementing a smaller pipe and incorporating two adaptors. In the simulation experiment, The power output of the Stirling engine experienced a rise from roughly 700W to 890W when the pipe diameter was reduced from 30mm to 12mm. However, there was a subsequent minor fall to 840W when the pipe diameter remained at 12mm, as illustrated in Figure 2.10.

According to the findings of this study, increasing dead volume reduces engine efficiency. The Stirling engine's efficiency with ideal regeneration and zero dead volume equals that of the Carnot cycle. However, in the actual scenario, it is different from the Carnot cycle, the Stirling engine is a practical engine that can actually be used to produce useful work (Kongtragool and Wongwises, 2006).

Another research done by Ricardo et.al also found that the efficiency of the Stirling engine is reduced due to the imperfect regeneration is strongly amplified by the dead volume (Beltr An-Chacon et al., 2015).

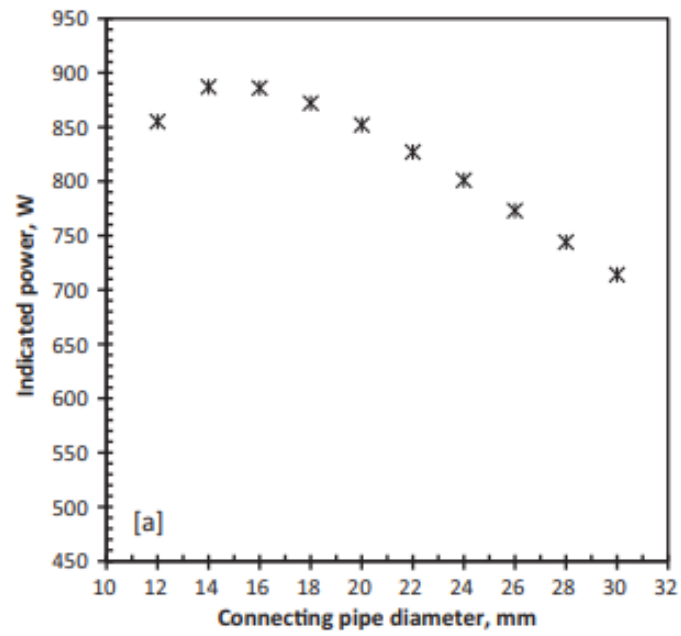


Figure 2.10: Influence of connecting pipe diameter on engine power performance. (Alfarawi, AL-Dadah, et al., 2016)

2.8 Matrix Conductivity and Heat Capacity of the Regenerator Effects on Stirling Engine's Performance

Table 2.2: Effect of the regenerator material on engine performance.(Timoumi et al., 2008)

Regenerator matrix metal	Volumetric capacity heat ($J/m^3 K$)	Conductivity ($W/m K$)	Engine power (W)	Engine effectiveness (%)	Exchanged energy in the regenerator (J)
Steel	3.8465×10^6	46	4258	38.84	441.25
Stainless steel	3.545×10^6	15	4273	39.29	448.72
Copper	3.3972×10^6	389	–	–	–
Brass	3.145×10^6	100	4080	34.6	415.67
Aluminum	2.322×10^6	200	3812	29.16	378.03
Granite	2.262×10^6	2.5	4091	34.51	430.75
Glass	2.1252×10^6	1.2	4062	33.85	427.8

In a study conducted by Timoumi et al., the study revealed that the Stirling engine's performance is influenced by the thermal conductivity and heat capacity of the material that makes up the regenerator matrix. The research revealed that an increase in the thermal conductivity of the regenerator matrix results in reduced performance due to heightened internal conduction losses within the regenerator. Moreover, the Stirling engine's performance is enhanced with an increase in the heat capacity of the regenerator matrix.

The construction of the regenerator matrix can be achieved using a variety of materials, as detailed in Table 2.2, which provides a comprehensive breakdown of the Stirling engine's performance based on the specific material employed. The choice of the regenerator matrix material directly affects the engine's performance. In order to enhance heat transfer efficiency within the regenerator and reduce internal losses resulting from conductivity, it is crucial to meticulously select a material characterized by high heat capacity and low thermal conductivity. According to the data shown in Table 2.2, stainless steel and ordinary steel emerge as the most appropriate materials for fabricating the regenerator matrix. (Timoumi et al., 2008).

2.9 Summaries Existing Studies from Review

Table 2.3 presents a comprehensive overview of the relevant studies identified in the literature research. The table contains a summary of the features, advantages, and disadvantages associated with each of the investigations.

Table 2.3: Summary of Existing Studies

No.	Journal	Summaries feature of the studies	Advantages	Disadvantages
1.	Phase angle effects on Stirling engine performance.	Studies were carried out with various phase angles to examine the performance of the Stirling engine.	One of the most effective methods for regulating the output of the Stirling engine.	Take time to tune the phase angle between the flywheels of the displacer piston and the working piston.
2.	Dead space effects on Stirling engine performance.	Experiments were conducted using varying sizes and diameters of the connecting pipe to assess the Stirling engine's performance.	It will help improve the performance of the Stirling engine.	Most of the marketed Stirling engines come with fixed connecting pipes, which almost impossible to change the diameter of it.
3.	Regenerator Matrix Conductivity and Heat Capacity Effects on Stirling Engine's Performance.	Experiments were conducted on the regenerator using various types of materials.	One of the most effective methods for regulating the output of the Stirling engine.	Most of the marketed Stirling engines come with a prebuilt regenerator, which makes it impossible to change the material.

2.10 Related Projects

2.10.1 Electricity Production In Rural Villages With A Biomass Stirling Engine

According to a study conducted by Podesser E, a Stirling engine heated by the flue gas from a biomass furnace is intended for generating electricity in rural areas without access to the grid. An α -type Stirling engine was chosen for its ability to utilize many components from industrial mass production. An experiment was conducted using the prototype Stirling engine in a testbed configuration with a wood chip furnace, and the results are presented in the table below. Table 2.4 reveals that the prototype's efficiency is quite high, approximately 0.25 (Podesser, 1999). Furthermore, the individual engine's size is quite large, making it unsuitable for mobility purposes.

Table 2.4: Test Results of Biomass Stirling Engine (Podesser, 1999)

Flue gas temp.	1.000	°C	Mean preassure	33 (40)	bar
Dust content	70 ... 700	mg/m ³ N	Bore/stroke	140/51	mm
Engine cooler	30 ... 70	°C	Swept piston volume	840	cm ³
Cylinder cooler	20 ... 30	°C	Compensator	17	liter
Rod seals cooler	20 ... 30	°C	Working speed	600	RPM
Thermal input	12,5	kW	Idling speed	950	RPM
Engine cooler	8,75	kW	Efficiency (COP)	0,25 ... 0,28	-
Cylinder coolers	0,52	kW	Crankmechanism	DUCATI 500	cm ³
Rod seals cooler	0,03	kW	Flyweel/starter	Austrian Truck	
Shaft power max.	3,2	kW	Working gas	air, nitrogen	

2.10.2 The Application Of An Innovative Integrated Swiss-roll-combustor On A Stirling Engine

A study conducted by Wu et al on the application of Swiss-roll-combustor Stirling engine. Figure 2.11 depicts a Swiss-roll-combustor Stirling engine and Figure 2.12 shows the diagram of the Swiss-roll combustor. The Swiss roll combustor is laden with small catalytic beads to decrease the ignition temperature and improve combustion efficiency (Li et al., 2013). From the research, Wu et al. found out that Swiss-roll-combustor provides a broader range of fuel/air ratio, improving the combustion efficiency. Besides that, the structural support from the spiral channel wall in the Swiss roll combustor enables the bottom wall of the Stirling engine to be made very thin, which improves the rate of heat transfer from the heat source to the engine. As more heat energy is transferred into the engine, more work will be produced through the engine cycle. As compared to the Stirling engine without the swiss-roll-combustor, the engine performance has been improved remarkably (Wu et al., 2021).

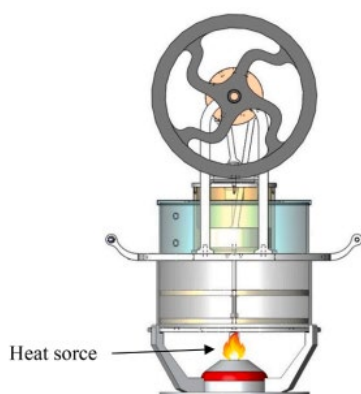


Figure 2.11: Swiss-roll-combustor Stirling Engine (Wu et al., 2021)

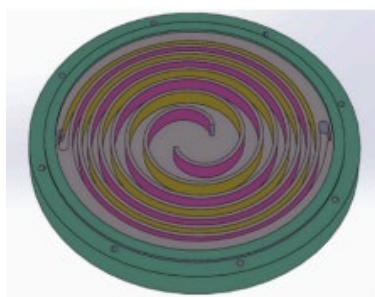


Figure 2.12: Swiss-roll-combustor (Wu et al., 2021)

2.10.3 Review On Solar Stirling Engine: Development and Performance

A study conducted by Singh et al. revealed that the solar dish-Stirling system is the most efficient method for generating electricity from solar energy. This study considered various parameters, such as concentration ratio, absorber temperature, hot side temperature, cold side temperature, regenerator effectiveness, working fluid, dead volume, and average working pressure, in the performance analysis of dish-Stirling systems. The researchers noted that increasing the concentration ratio leads to higher absorber temperature and improved thermal efficiency. The energy efficiency of the dish-Stirling system was reported to be 17%, with the primary losses occurring at the receiver. The results demonstrate that dish-stirling technology can cost-effectively produce power with better performance compared to other renewable systems (Singh and Kumar, 2018).

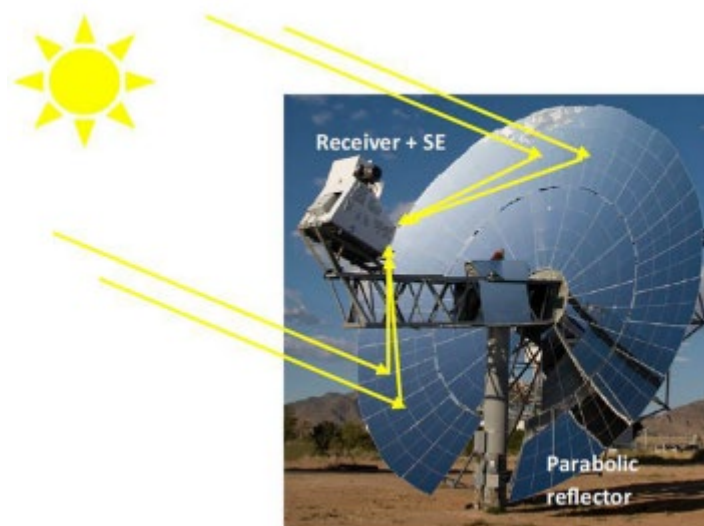


Figure 2.13: Dish-Stirling engine with different components (Singh and Kumar, 2018)

Kadri et al. also performed an analysis on the performance of the standalone dish-Stirling system for off-grid electricity generation in rural areas. A model was developed for a standalone dish-Stirling with permanent magnet synchronous generator system to study the feasibility of the arrangement. It was concluded that a variable speed system would be a good choice for feeding an uncontrollable load (Kadri and Hadj Abdallah, 2016). Nonetheless, the dish-Stirling technology encounters several challenges. Foremost among these is the issue of shading. In regions with a low solar altitude angle, particularly during the winter in countries with four distinct seasons, losses due to shading effects are heightened. Therefore, a comprehensive shading analysis should be conducted to address this concern (Zilanll and Eray, 2017).

In addition to this, the presence of moving parts in the dish-Stirling engine can result in wear and tear of system components, potentially leading to system shutdown. In contrast, solar PV systems are not susceptible to such issues. To ensure reliability, it is imperative to make precise predictions regarding radiation flux and temperature distributions on the tube walls of the Stirling engine heater head (Li et al., 2011).

2.11 Summary

Throughout this chapter, the diverse working principles and performance characteristics of the Stirling engine have been discussed. Moreover, the operational mechanisms of different types of Stirling engines have also been examined, along with their performance. The system's concept has also been discussed in this chapter. Furthermore, factors that affect the performance of the Stirling engine have also been reviewed.

CHAPTER 3

METHODOLOGY AND WORK PLAN

3.1 Introduction

The primary aim of this project is to establish a miniature Stirling engine charging system. Additionally, the project seeks to analyze and compare the output voltage of the DC generator and evaluate the maximum achievable power of the Stirling engine. This chapter will elucidate and deliberate on the method, selection of components, electrical design, system design, setup, and the processes employed to successfully accomplish the project. Beforehand, a Stirling engine must be designed and built based on reference.

Initially, the project's flow was deliberated over through the utilization of a flowchart. Subsequently, an extensive amount of research was conducted on the material and components employed. In addition to the aforementioned points. The configuration of the framework and the electrical architecture of the charging system were also explained and deliberated about. Furthermore, a comprehensive demonstration and thorough explanation of the system's performance analysis methodology were provided.

3.1.1 Development Methodology

The project utilizes the development cycle technique as illustrated in Figure 3.1. The project will be divided into several stages, each with specific objectives, spanning from the initial ideation to the final launch. The iterative process will be iterated until the prototype has effectively attained the predetermined objectives, encompassing ideation and requirement generation, component delineation, aesthetic design, testing, and deployment. The prototype is prepared for deployment subsequent to the successful attainment of the predetermined objectives and requirements.

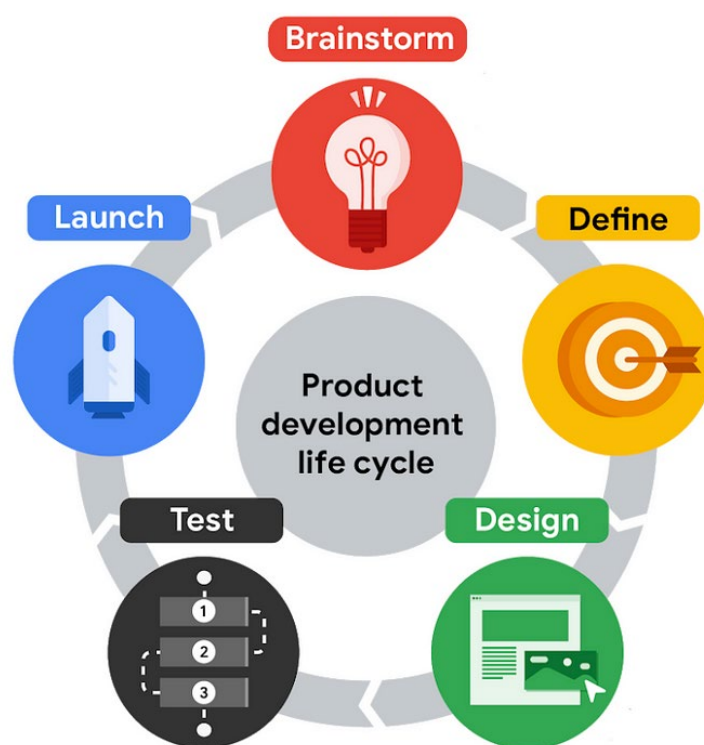


Figure 3.1: Product development life cycle

3.2 Process Flowchart

A flowchart was prepared prior to the commencement of the project in order to furnish a concise framework and enhance comprehension during the project's initiation. The process flowchart of the proposed project is depicted in Figure 3.2.

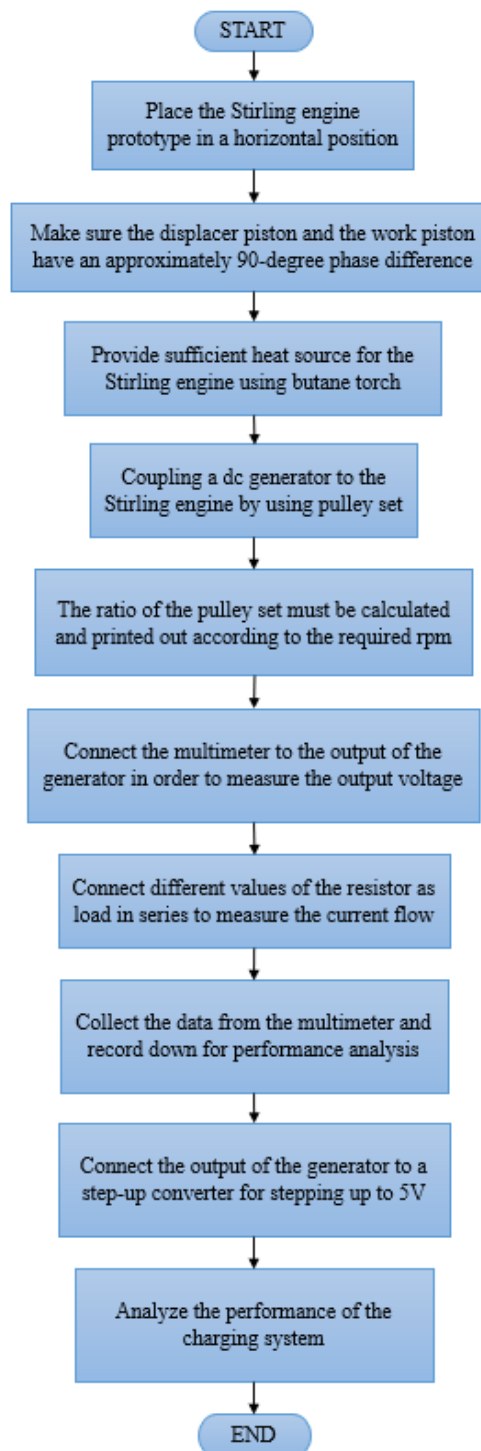


Figure 3.2: Process Flowchart

3.3 Engine Manufacturing

The first-generation Gamma Stirling engine has been successfully assembled with the assistance of Prof. Lim Yun Seng and extensive references. It was constructed in the KB block Engineering Mechanical Workshop as shown in Figure 3.3 and Figure 3.4, and subsequent testing and modifications were carried out at personal facility, indicating a hands-on and practical approach to the project. The engine's composition includes the heater, crafted from steel, the displacer piston section, constructed from stainless steel sheet and titanium sheet with a thickness of 0.05mm, and the flywheels crafted from cast iron by using the lathe machine located in the workshop. All these materials were chosen for their contributions to the engine's structural integrity and functionality.

The engine has been tested using air as a working fluid and butane gas as fuel. This implies versatility in its applications, as different working fluids and fuels can have varying effects on the engine performance.



Figure 3.3: Bend saw to cut the metal bar



Figure 3.4: Lathe machine to obtain the required diameter of the metal cylinder

3.4 System Setup

A Gamma-type Stirling engine was built based on several references and subjected to modest adjustments, specifically about the phase difference between the displacer piston and the working piston, as well as the lubrication of the pistons. These modifications were undertaken with the aim of optimizing the performance of the Stirling engine to the greatest extent feasible. The system comprises a direct current (DC) motor generator, a custom printed pulley set, a Stirling engine speed regulator, a step-up converter, and an onboard 5V USB-female chip. The coupling of the DC motor generator to the Stirling engine is achieved by the utilization of a pulley set as shown in Figure 3.5, Figure 3.6, and Figure 3.7. The step-up converter is employed to amplify the generated voltage to a stable level of 5V in order to facilitate the USB output. In addition to that, an external cooling system is added to the setup to effectively lower the temperature of the cold side of the regenerator heat exchanger. This external cooling system comprises several components, including a cooling fan, a rectangular radiator, a water pump, and a network of piping. This setup ensures efficient cooling of the regenerator's cold side, maintaining optimal operating conditions for the system. Figure 3.8 and Figure 3.9 depict the essential components necessary for the cooling system and ways by which the cooling system is integrated into the system.

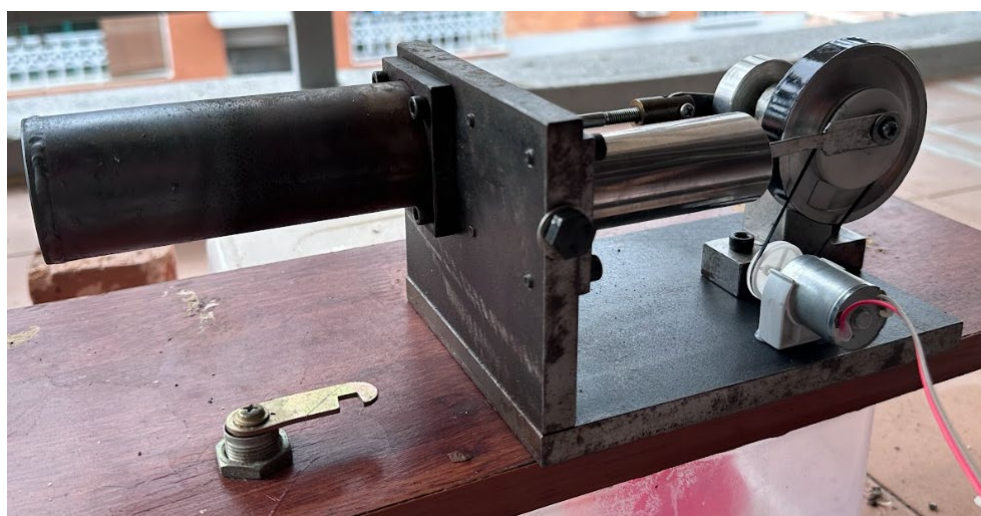


Figure 3.5: Setup of Stirling engine prime-mover

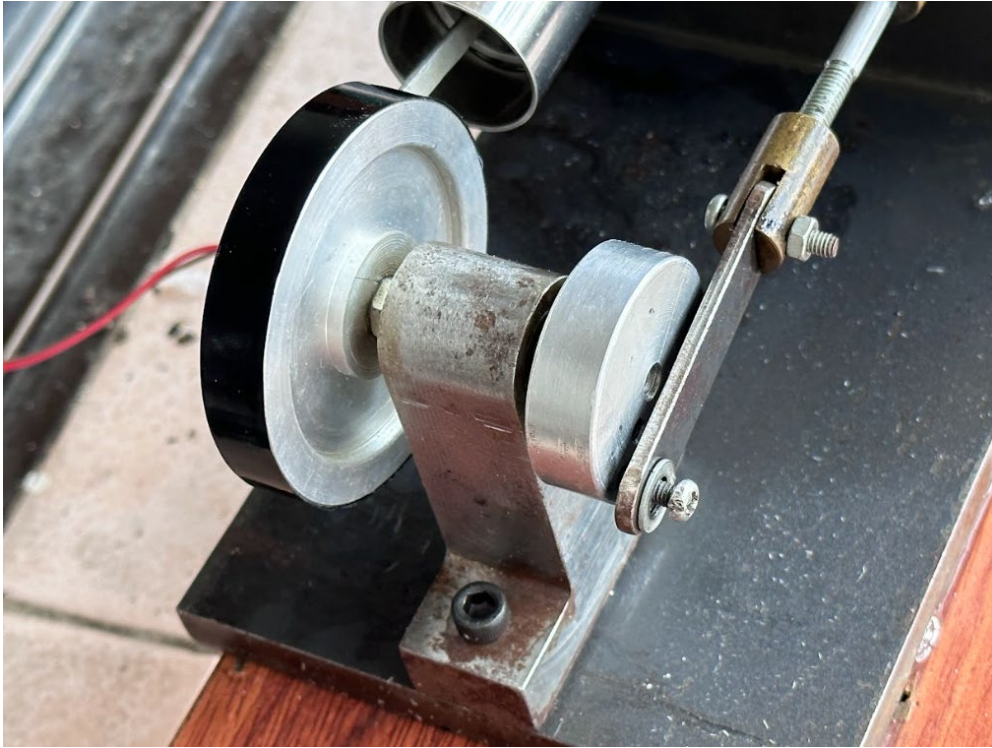


Figure 3.6: Flywheel of Stirling engine

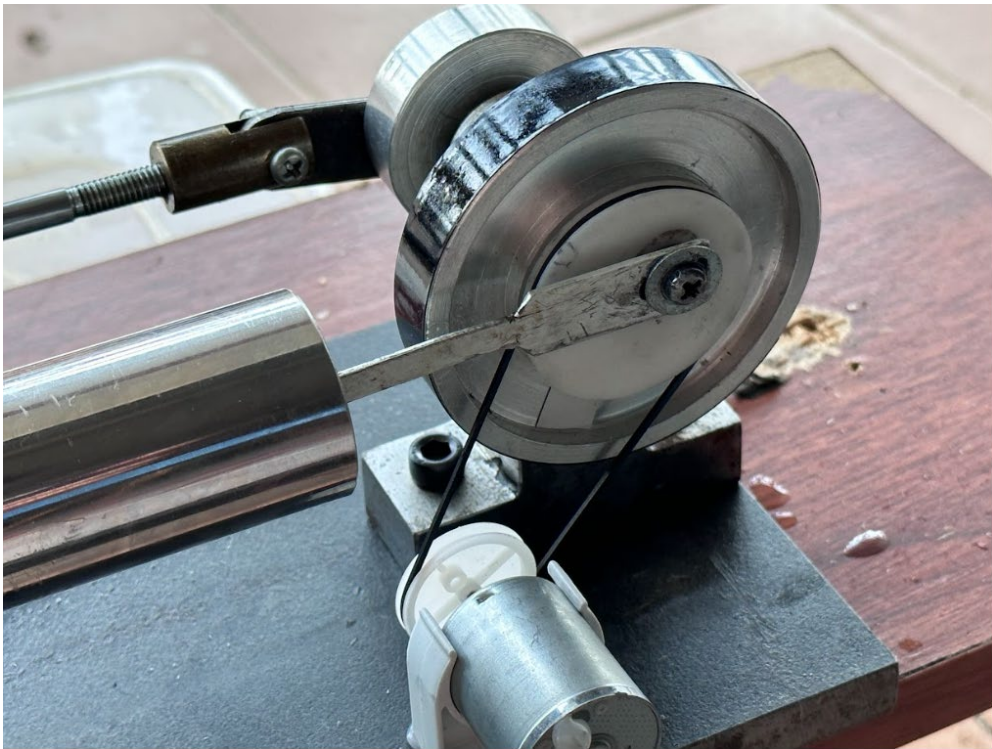


Figure 3.7: 3D-printed coupling pulley-set

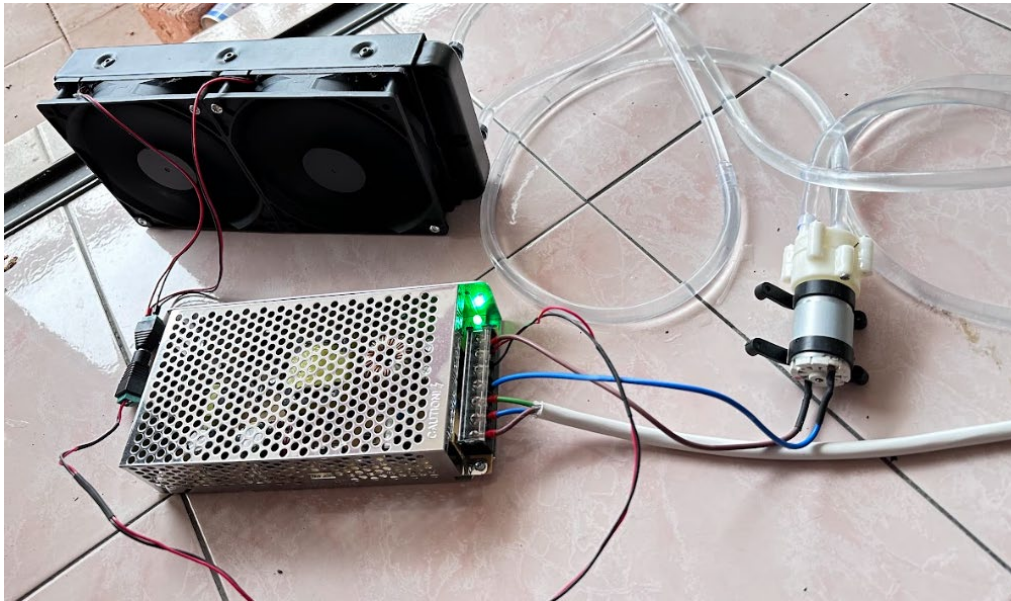


Figure 3.8: Cooling system components



Figure 3.9: Cooling system attached to the Stirling engine

3.4.1 Electrical Connection of the Charging System

Figure 3.10 shows the connection of the system. For this project, the RF-370 DC motor generator was used. The RF-370 DC generator was connected to the flywheel of the Stirling engine by using the pulley system. The positive terminal and negative terminal of the DC generator were connected to the input of the speed regulator and DC-DC boost converter respectively according to the order. After that, a USB type-A female jack module was then connected to the output of the DC-DC boost converter in order to power up or charge up mobile devices.

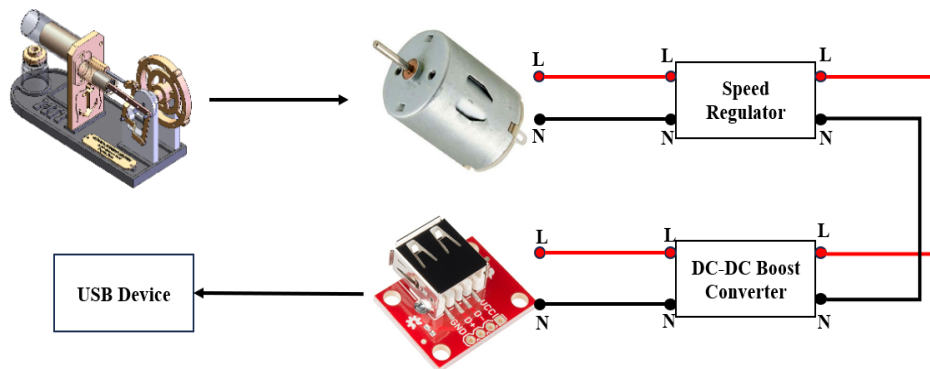


Figure 3.10: Connection of charging system

3.5 Tools

In general, a project often necessitates a range of hardware elements and components. Research is conducted on the most crucial and noteworthy components utilized in the project. The research encompasses an examination of several categories of DC motor generators, an exploration of DC-DC boost converters, and an analysis of the pulley system's architecture.

3.5.1 RF-370 DC Motor Generator

Figure 3.11 shows the DC generator used in this proposed project. The charging system configuration utilizes a DC motor generator depicted as RF-370, which functions as the direct current (DC) generator. The maximum achievable output voltage of this generator is approximately 12V. The RF-370 DC generator is capable of generating a no-load output voltage of roughly 4V when operated at an optimal rotational speed of 1055 RPM. Nevertheless, the flywheel of the chosen Stirling engine model lacks the ability to rotate at such elevated velocities. Therefore, it is necessary to design a pulley system in accordance with the specified requirements by utilizing an online pulley simulation. The selection of the RF-370 DC motor generator for this project is based on its low turning torque and the fact that its shaft diameter matches the required size.



Figure 3.11: DC motor RF-370

Table 3.1: Features of RF-370 DC Motor Generator

Rated Speed	200RPM – 6000RPM
Output Current	0.01 A – 0.2A
Output Voltage	0.1V – 22V

3.5.2 Online Pulley Simulation

To get an approximate output of 4V, it is necessary for the Model 300 DC generator to operate at a rotational speed of approximately 1055 rpm. The smaller pulley, which is connected to the DC generator, has a diameter of 24 mm. The measured reading obtained from the tachometer indicates that the Gamma Stirling engine's flywheel achieves an approximate steady-state speed of 630 revolutions per minute (rpm). According to the pulley simulation conducted online, the diameter of the pulley that is connected to the flywheel of the Stirling engine has been determined to be 40 mm.

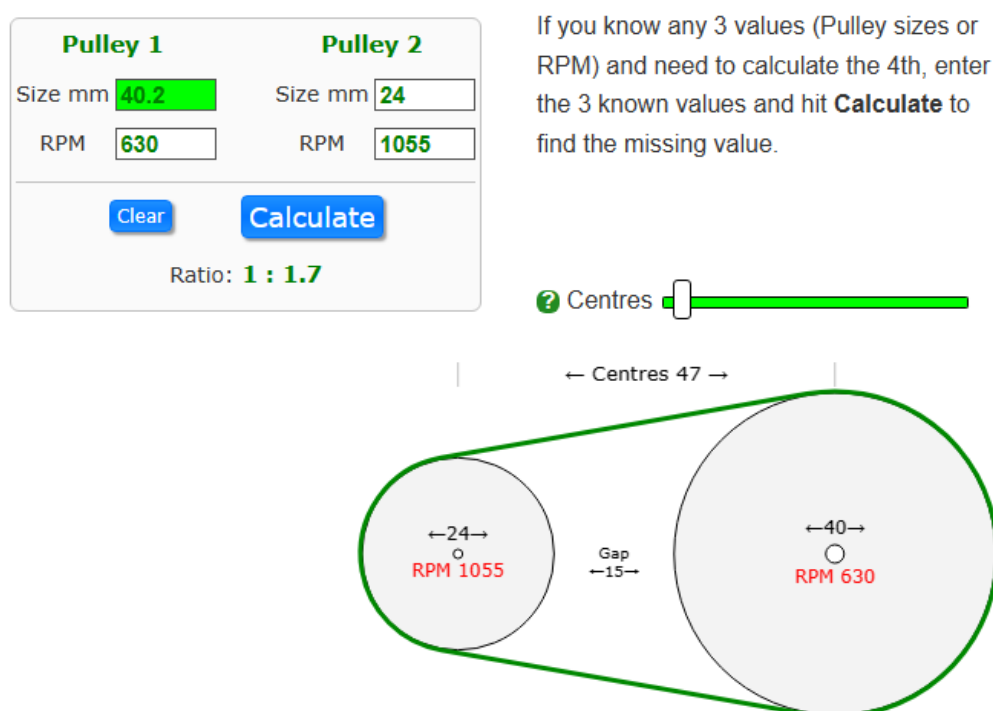


Figure 3.12: Pulley simulation

The calculation performed by the simulation is depicted in Figure 3.12, revealing that a pulley size of 40 mm, when coupled to the flywheel of the Stirling engine, is necessary to provide an output voltage of around 4 volts.

3.5.3 Stirling Engine Speed Regulator

A Stirling engine speed regulator is built as shown in Figure 3.13 and implemented within the system to govern the rotational speed of the Stirling engine, ensuring its optimal operation. While the primary goal of the speed regulator is often associated with achieving the desired maximum output power, its function extends beyond this singular objective. Alongside optimizing power output, the speed regulator plays a pivotal role in maintaining efficiency by keeping the engine within its optimal speed range. Moreover, it facilitates the engine's ability to adapt to varying loads or power demands, ensuring stable and controlled operation. Through continuous monitoring and adjustment of the engine speed, the regulator enhances overall system performance while safeguarding against mechanical stress or inefficiencies. Thus, the speed regulator serves as a critical component in coordinating the efficient and reliable operation of the Stirling engine within a broader framework of power generation or utilization.

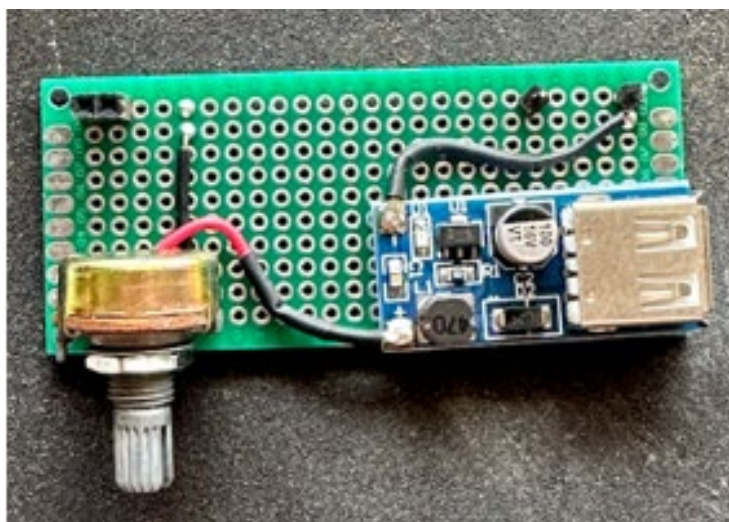


Figure 3.13: Speed Regulator

3.5.4 DC-DC Boost Converter

A DC–DC boost converter, also known as a step-up converter, is an electronic circuit that converts a lower-voltage DC input into a higher-voltage DC output. This type of converter is widely used in various applications where it is necessary to increase the voltage level while maintaining the same polarity. Figure 3.14 shows the HT7750 DC-DC boost converter that used in this project.

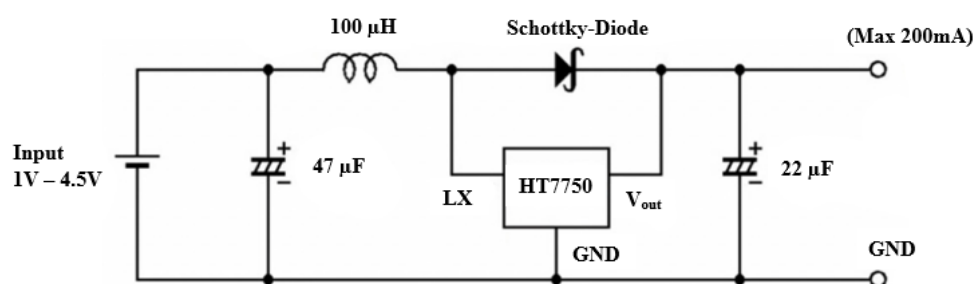


Figure 3.14: DC-DC Boost Converter

The DC-DC boost converter is utilized in the proposed project, as indicated by the features outlined in Table 3.2. The utilization of this particular DC-DC boost converter in the project is justified due to its reduced start-up voltage compared to alternative converters, as well as its ability to deliver high precision in output voltage. Furthermore, the main core of the converter used is the HT7750/ SOT23 series module, it provides high efficiency and low ripple. It requires only three external components which include capacitors, inductors, and a Schottky-diode that is employed to establish a constant output voltage at levels of 1.8V, 2.2V, 2.7V, 3.0V, 3.3V, 3.7V, 5V, or 10V. CMOS technology ensures ultra-low supply current and makes them ideal for low-power applications. Figure 3.15 shows the actual circuit of the DC-DC boost converter. Table 3.3 shows the features of HT7750/ SOT23. Figure 3.16 shows the HT7750/SOT23 that used in the proposed project. In addition, Figure 3.17 illustrates the pin arrangements of HT7750/ SOT23.

Table 3.2: Features of DC-DC Boost Converter

	DC-DC Boost Converter
Input voltage range, V	1V – 4.5V
Maximum output voltage, V	+10V
Maximum output current, A	+200mA

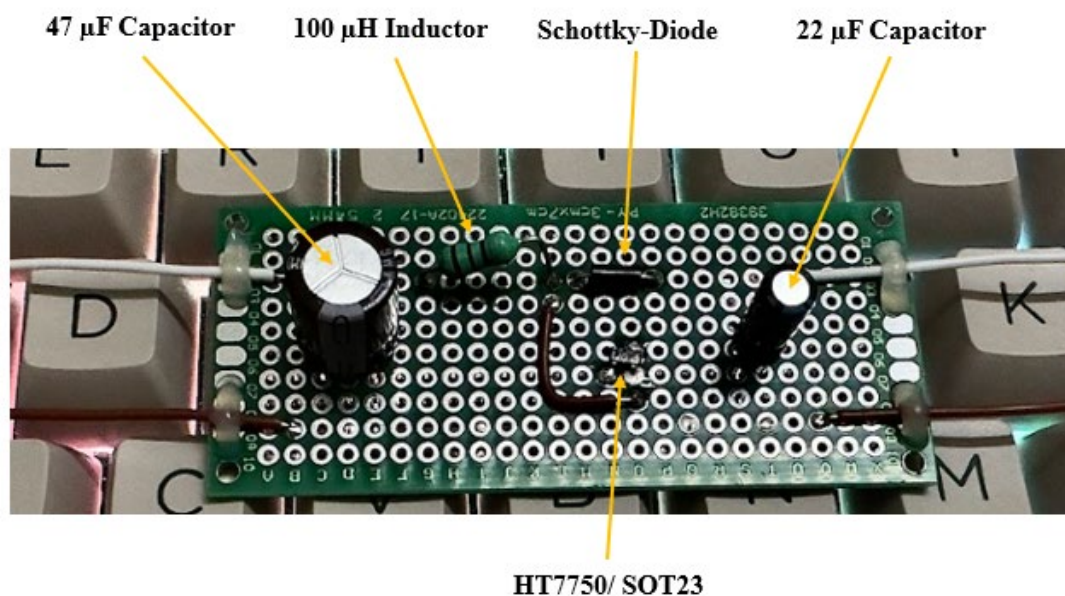


Figure 3.15: Circuit of DC-DC boost converter

Table 3.3: Features of HT7750/ SOT23 Converter

	HT7750/ SOT23
Low start-up voltage, V	0.7V
Output voltage, V	1.8V, 2.2V, 2.7V, 3.0V, 3.3V, 3.7V, 5.0V, 10V
High efficiency, %	85%

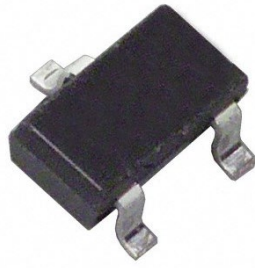


Figure 3.16: HT7750/ SOT23

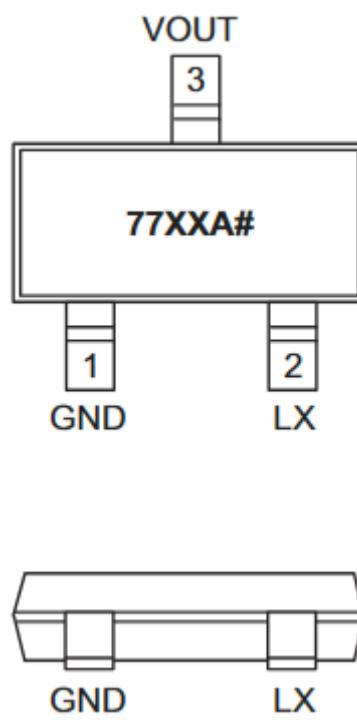


Figure 3.17: Pin Configuration of converter HT7750/ SOT23

3.5.5 12V DC Brushless Cooling Fan

Figure 3.18 shows the 12V DC brushless cooling fan. In the intricate mechanics of this proposed project, this fan serves a pivotal role. Its primary objective is to optimize the airflow within the system, thereby facilitating the effective cooling of the water cooling system embedded within the Stirling engine setup. By increasing the circulation of air, these fans play an important role in maintaining the optimal operating temperature of the entire system. In order to ensure effective cooling capabilities, two 12V DC brushless cooling fans have been incorporated into the project design, working in tandem to achieve the desired cooling efficiency.



Figure 3.18: 12V DC Brushless Cooling Fan

3.5.6 Liquid Cooling Radiator

Figure 3.19 illustrates the liquid cooling radiator that is used in the proposed project. It serves the important function of dissipating excess heat generated during the Stirling engine's operation. In the continuous working of the Stirling engine, heat management is paramount for optimal performance and longevity. As the Stirling engine operates, heat is generated as a natural byproduct of the thermodynamic processes involved in converting thermal energy into mechanical work. The liquid cooling radiator acts as a heat exchanger, efficiently transferring the heat absorbed by the engine to a liquid coolant circulating through its internal channels. Once the hot coolant absorbs the heat from the engine cylinder, it is then circulated away from the engine and into the liquid cooling radiator. Within the radiator, hot coolant releases its heat to the surrounding air through a series of fins and tubes, aided by airflow generated by the 12V DC brushless cooling fan. As the coolant cools down, it is then recirculated back to the engine to repeat the cooling process, creating a continuous cycle of heat dissipation.



Figure 3.19: Liquid Cooling Radiator

3.5.7 12V DC Pneumatic Diaphragm Water Pump

In the Stirling engine water cooling radiator system, a water pump plays a crucial role in ensuring efficient cooling of the engine. Figure 3.20 shows the 12V DC pneumatic diaphragm water pump. It serves as the primary means of circulating coolant fluid throughout the water cooling system. The 12V DC pneumatic diaphragm water pump facilitates the circulation of the coolant fluid within the system. When activated, the pump draws coolant from a reservoir, creating a suction effect that pulls the coolant fluid into the pump chamber. The diaphragm's reciprocating motion, driven by the 12V DC power supply, alternately expands and contracts, creating pressure differentials that propel the coolant liquid through the water cooling system.



Figure 3.20: 12V DC Pneumatic Diaphragm Water Pump

3.5.8 12V DC Power Supply

Figure 3.21 shows the 12V DC power supply. In the Stirling engine water cooling system, a 12 V DC power supply is essential for powering various components including the 12V DC cooling fan, and the 12V DC pneumatic diaphragm water pump.



Figure 3.21: 12V DC Power Supply

3.5.9 SolidWorks

In this proposed project, SolidWorks software serves as the primary tool for designing the prototype's pulley system. Solidworks is a robust and extensively employed computer-aided design (CAD) software application developed by Dassault Systemes. It finds its primary use in 3D modeling, simulation, and engineering design. Engineers, architects, and product designers favor SolidWorks for its potent capabilities and user-friendly interface. Whether users are creating mechanical components, architectural structures, or intricate machinery, Solidworks can streamline the design process and boost productivity. The detailed schematics and drawings of the SolidWorks are presented below as Figure 3.22. Figure 3.23 depicts the logo of SolidWorks.

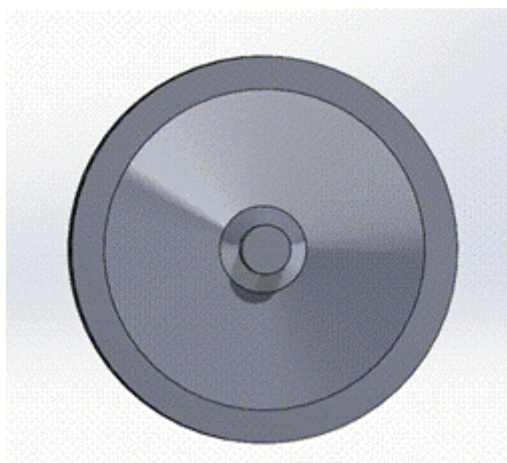


Figure 3.22: Pulley Designed

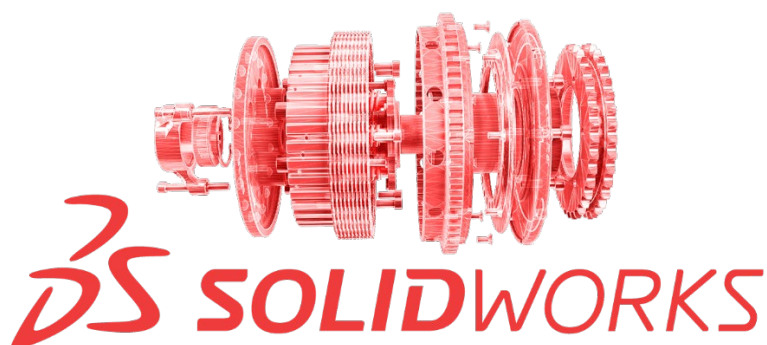


Figure 3.23: Logo of SolidWorks

3.6 Summary

This chapter offers a thorough explanation of the required hardware and software components of the Stirling engine and its generator. It delves into the integration techniques for incorporating these components into both the charging system and the external water cooling system, highlighting their interconnections. Each component is integrated into the system with careful consideration for potential scaling and expansion, ensuring readiness for future requirements.

CHAPTER 4

RESULTS AND DISCUSSION

4.1 Introduction

The integration of the Stirling engine with the DC generator charging system has been successfully established, and the ensuing chapter will delve into the discussion of the results. These results have been compiled from various tests conducted with different load resistances and minor changes in the characteristics of the Stirling engine including the phase angle between the flywheels, the material of the displacer piston, and the diameter of the displacer piston. Additionally, the power output of the Stirling engine will be assessed and discussed. Furthermore, this chapter will also explore the challenges faced by the Stirling engine in achieving its maximum performance and the challenges confronting the entire charging system in operating at its peak efficiency.

4.2 Measuring System

Before commencing the experiment, the measurement system is set up using two multimeters. To measure both the output voltage drop and output current flow of the DC generator when driven by the Stirling engine, the DC generator is connected in series with a variable resistor. This configuration allows for the measurement of both the voltage across the variable resistor and the variations in current flow through it. Two multimeters are employed for this purpose. The first multimeter is interconnected in a series configuration within the circuit in order to measure the magnitude of electric current passing across the entirety of the circuit. Meanwhile, the second multimeter is connected in parallel across the variable resistor to measure the voltage drop across it. Once the Stirling engine is started, the generator energizes the circuit. Throughout this process, both multimeters continuously capture and display real-time data while changing the value of the variable resistor. These readings are noted down for subsequent analysis and graph plotting.

To summarize, the inclusion of two multimeters in the setup serves the purpose of conducting a thorough evaluation of the DC generator's performance when driven by the Stirling engine. The data recorded by these instruments play a pivotal role in examining how voltage and current fluctuate in response to variations in the resistance of the variable resistor. This, in turn, contributes significantly to gaining valuable insights into the findings related to the output power of the DC generator.

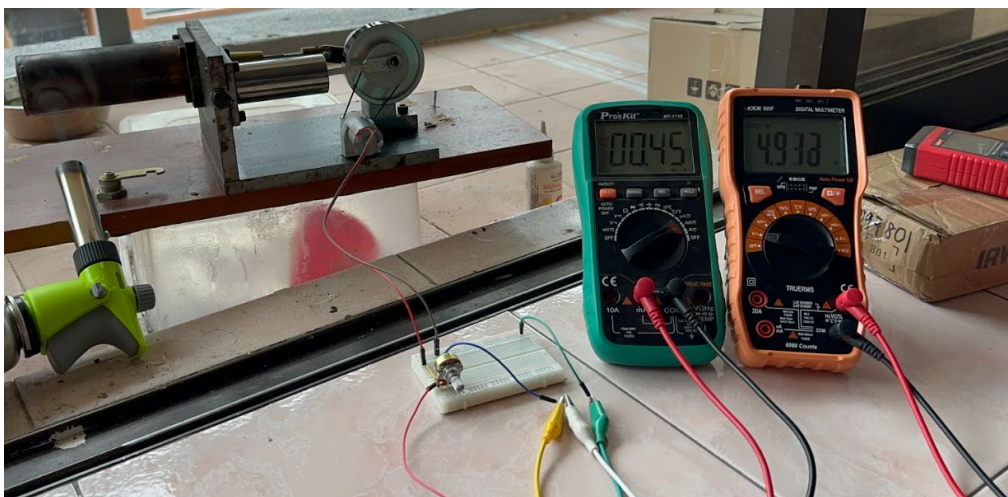


Figure 4.1: Measurement system

4.3 Output Power of the System

4.3.1 Aluminium Displacer with Diameter of 39mm (90° phase angle)

Figure 4.2 provides a detailed representation of the relationship between the current flow in the circuit and the voltage drop across the variable resistor. Initially, when the variable resistor is adjusted to its minimum resistance, the voltage drop across it is the lowest, measuring approximately 0.129V. Correspondingly, the current flow in the circuit is measured at 0.03527A under these initial conditions. This higher current flow is expected because, with lower resistance in the circuit, electrons can move more freely, thus resulting in a higher current flow. However, with each increment in resistance, the voltage drop across the variable resistor also increases. This behavior signifies that the resistor increasingly obstructs the flow of electric current, leading to a more significant voltage drop.

Conversely, the current flow in the circuit exhibits a decreasing trend. As the resistance of the variable resistor rises, the current flowing through the circuit decreases gradually. This is consistent with Ohm's law, which states that the current in a circuit is inversely proportional to the resistance.

Furthermore, when the variable resistor is set to its maximum resistance value, which is 10k Ω , the voltage drop across it reaches its peak at approximately 5.658V. At this point, the resistor is acting as a significant barrier to the flow of electricity, resulting in a substantial voltage drop. Concurrently, the current flow in the circuit reaches its lowest point, measuring 0.00052A. This minimal current flow is a direct consequence of the high resistance encountered in the circuit, effectively limiting the current flow.

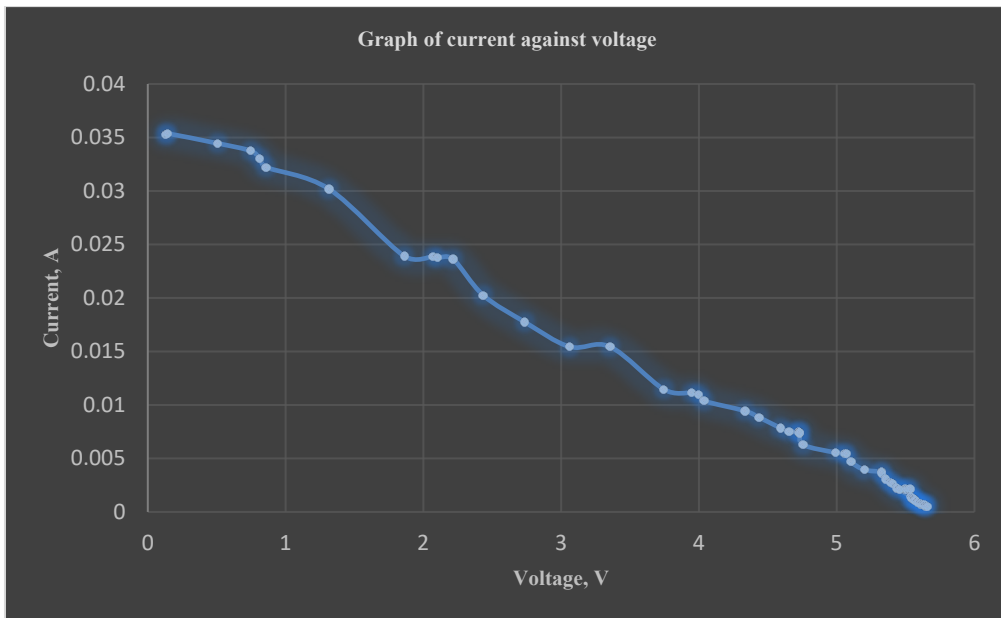


Figure 4.2: Graph of current against voltage across the variable resistor

The graphical representation in Figure 4.3 illustrates the relationship between the power output of the DC generator and variations in voltage across the variable resistor. According to the data presented in Figure 4.3, it is evident that the DC generator achieves its peak power output, approximately 0.0523626 watts, at a specific point. The graph in Figure 4.3 below clearly demonstrates that the DC generator's output reaches its highest level when the voltage across the variable resistor is maintained at approximately 2.215 volts. Conversely, as the resistance of the variable resistor is increased beyond this point, the output power of the DC generator experiences a decline. This information is crucial for comprehending the optimal operating conditions of the DC generator chosen for this project. Therefore, in order to optimize the output power of the DC generator, it is imperative to ensure that the voltage across the variable resistor remains at a value of roughly 2.2V. If the voltage across the variable resistor deviates from the recommended voltage drop, the power output of the DC generator will begin to decrease.

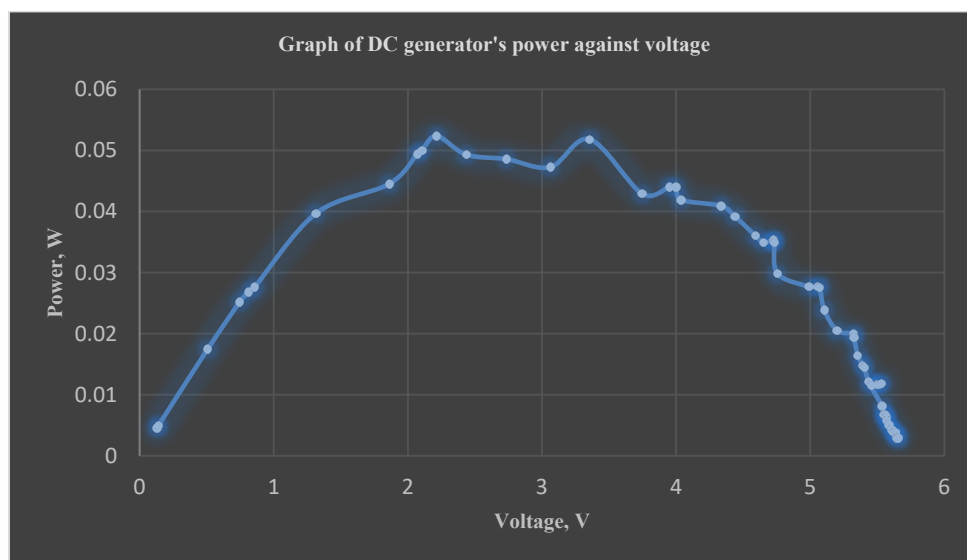


Figure 4.3: Graph of DC generator's power against voltage across variable resistor

The graph presented in Figure 4.4 illustrates the correlation between the rotational speed of the flywheel in a Stirling engine and the corresponding voltage drop across the variable resistor. Based on the graphical representation, it can be concluded that there exists a direct proportionality between the voltage drop across the variable resistor and the speed of the flywheel. When the variable resistor is set to its smallest resistance, the voltage drop across it is observed to be the lowest, measuring roughly 0.141 V. Additionally, the rotational speed of the flywheel under this particular circumstance is estimated to be around 372 rpm. This phenomenon occurs due to the inverse relationship between the resistance of a variable resistor and the current flowing through it. When the resistance of the variable resistor reaches its minimal value, the corresponding current flow across it reaches its highest magnitude. There exists a direct proportionality between the torque and the current flow. Therefore, when the current flow increases, there is a corresponding rise in the torque demanded by the DC generator. The consequence of this phenomenon is a deceleration of the speed of the Stirling engine, as the torque exerted by the Stirling engine is used to rotate the DC generator, hence slowing down its own speed.

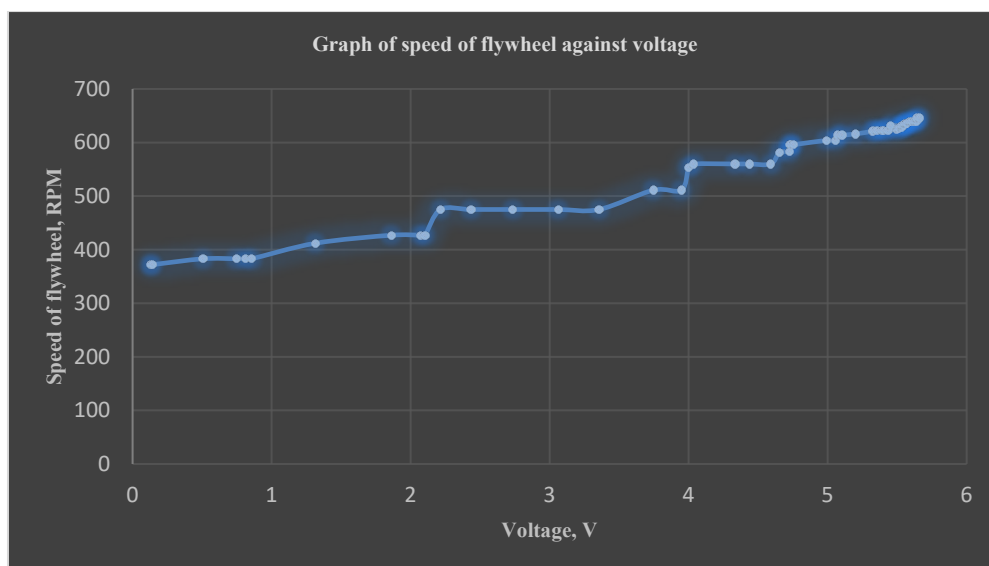


Figure 4.4: Graph of speed Stirling engine's flywheel against voltage across variable resistor

As illustrated in Figure 4.3, it is imperative to uphold a voltage drop of approximately 2.2 V across the variable resistor to achieve the utmost power output from the DC generator. To facilitate the DC generator in operating at its pinnacle of performance, namely generating an approximate output power of 0.05W, it becomes imperative to sustain the rotational speed of the Stirling engine within the specified range of 400–500 rpm, as exemplified in Figure 4.4. In summary, to regulate the rotational speed of the Stirling engine within the prescribed 400–500 rpm range, it is essential to maintain a voltage drop of roughly 2.2 volts across the variable resistor.

4.3.2 Titanium Displacer with Diameter of 39mm (90° phase angle)

A different material, a titanium sheet with a thickness of 0.01mm, is used to make the displacer piston. Following this, the previous measurement procedure is repeated to observe the performance of the modified Stirling engine. Graphs were plotted using the data collected on the performance of the modified Stirling engine.

Figure 4.5 illustrates the relationship between the current flow across the variable resistor and the voltage drop across it. Initially, when the variable resistor is set to its smallest possible value, calculated to be approximately 2.8Ω , the current flow across it reaches its peak, around 0.041A. Correspondingly, the voltage drop across the variable resistor is at its lowest, approximately 0.112V. As the variable resistor is adjusted to a larger value, the current flow across the circuit begins to decrease, while the voltage drop across the variable resistor starts to increase. This behavior is explained by Ohm's Law, $V = IR$, where resistance (R) is inversely proportional to current (I), and directly proportional to voltage drop (V).

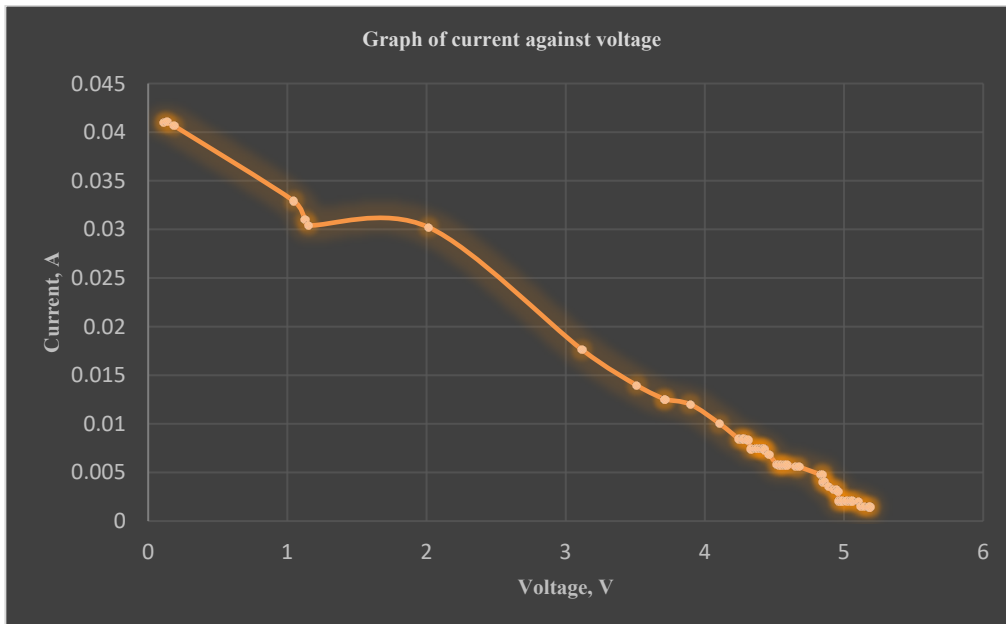


Figure 4.5: Graph of current against voltage

Figure 4.6 shows the graph of the output power of the DC generator against the voltage drop across the variable resistor of the modified Stirling engine using the titanium sheet as material to build the displacer piston.

Upon observing the data depicted in Figure 4.6, it can be distinguished that a nuanced yet noteworthy enhancement in the maximum power achievable by the DC generator compared to the predecessor Stirling engine, in which the displacer piston is built using the aluminum sheet. This advancement arises from the natural characteristics of using a titanium displacer, which is lighter than the aluminum displacer. This is because a lighter displacer piston imposes less resistance to movement, resulting in smoother engine operation and more effective energy conversion. Titanium's superior strength-to-weight ratio renders it an optimal choice, reducing piston mass without compromising the displacer piston's structural integrity. The observed rise in maximum achievable output power, from approximately 0.051W with the aluminum displacer piston to 0.061W with the titanium displacer piston, which is 0.01W slightly more power than the aluminum displacer piston Stirling engine. The shift from an aluminum to a titanium displacer piston has yielded a quantifiable enhancement in the Stirling engine's power output. This emphasizes the critical role of material selection and optimization in driving performance and efficiency in engineering systems.

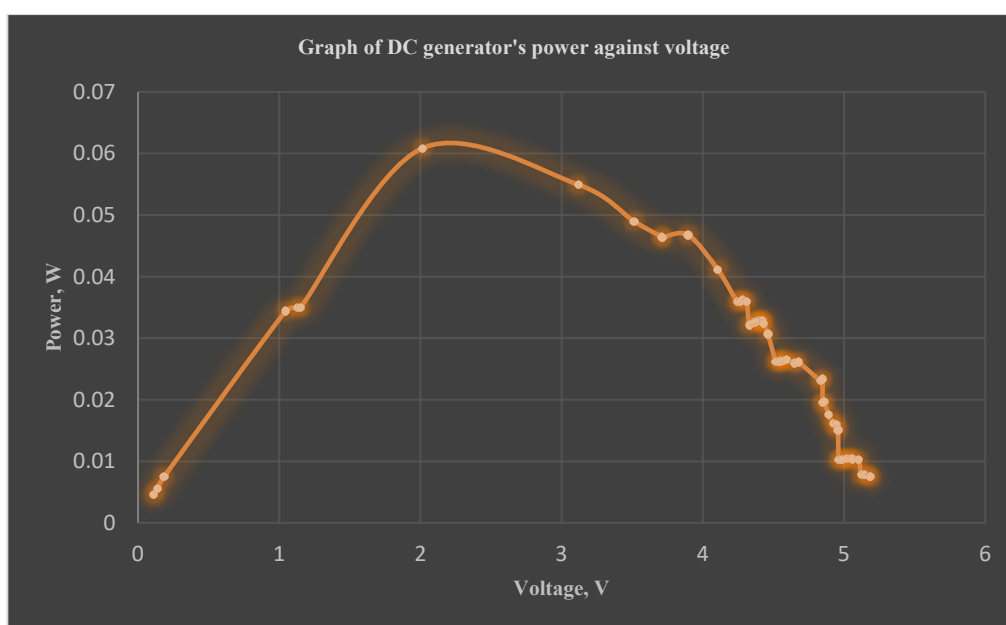


Figure 4.6: Graph of DC generator's power against voltage

The graph depicted in Figure 4.7 illustrates the relationship between the rotational speed of the flywheel and the voltage drop across the variable resistor. According to the data from Figure 4.7, in order to maintain the output power of the Stirling engine at its optimal level, it is crucial to maintain the voltage drop across the variable resistor at around 2V. Additionally, it is essential to sustain the rotational speed of the flywheel of the Stirling engine at approximately 500rpm to obtain optimal performance. Ensuring the voltage drop remains around 2V is integral to maintaining the Stirling engine's efficiency and performance. Similarly, maintaining the rotational speed at around 500rpm ensures that the engine operates within its most effective range. Achieving and preserving these parameters requires precise adjustment of the speed regulator to the correct position.

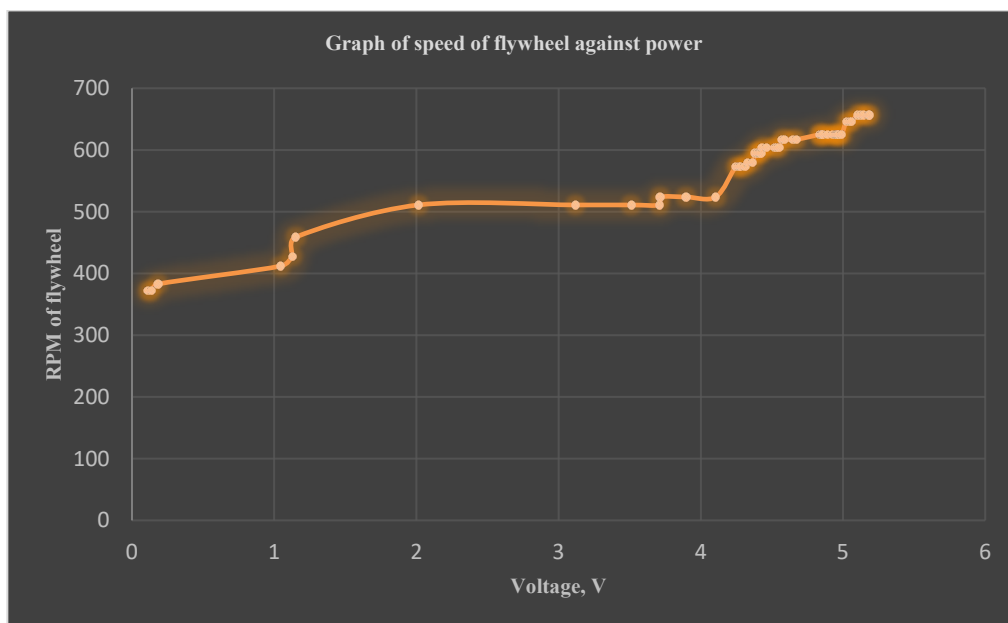


Figure 4.7: Graph of speed Stirling engine's flywheel against voltage across variable resistor

For the Stirling engine with a titanium displacer piston, the rotational speed of the flywheel and the voltage drop across the variable resistor are kept consistent with those of the Stirling engine featuring an aluminum displacer piston, but with an increase in the output power of the titanium displacer piston Stirling engine. While this improvement may seem minor, it represents an enhancement over the previous version.

4.3.3 Titanium Displacer with Diameter of 35mm (90° phase angle)

Figure 4.8 below shows the graph representing the relationship between current flow across the variable resistor and voltage drop across the variable resistor in a Stirling engine system, using a titanium displacer with a smaller diameter (35mm) compared to the previous two models. The flywheel maintains a 90-degree phase angle.

From the graph, it is evident that the current flow generated in the system is significantly lower compared to the previous two models. The maximum current observed is approximately 0.028A, corresponding to a voltage drop of 0.08V. As the resistance of the variable resistor increases, there is a rapid decrease in the current flow to approximately 0.01A. This decline continues steadily as the resistance of the variable resistor further increases. Conversely, the voltage drop exhibits an increasing trend with the rise in resistance. This suggests a clear inverse relationship between current flow and resistance, with voltage drop showing a direct correlation with resistance levels.

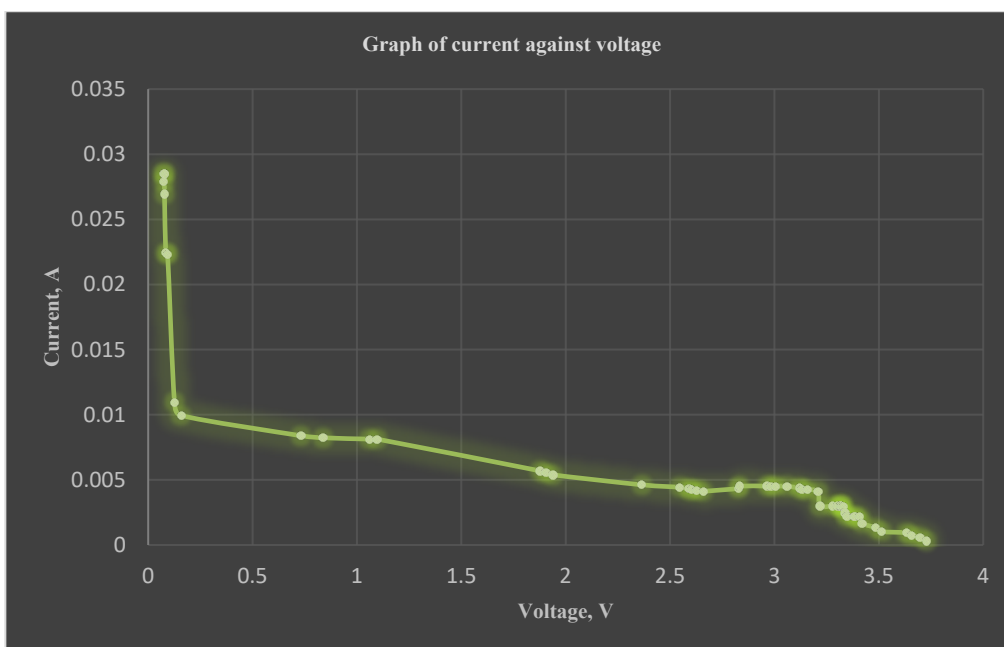


Figure 4.8: Graph of current against voltage

Figure 4.9 shows the graph of the DC generator's power against voltage drop across the variable resistor of the modified Stirling engine using a smaller diameter (35mm) of titanium displacer piston. From the graph, it can be observed that the generated output power of the Stirling engine is far lower than the previous model. This is because the displacement volume of the Stirling engine has reduced, although the weight of the displacer piston is lighter than the previous 39mm in diameter displacer piston. The displacer piston is responsible for transferring the working fluid (in this case gas is used) between the hot and cold zones of the Stirling engine. A smaller diameter displacer piston means a smaller volume of working fluid is displaced during each cycle. Hence, this reduces the amount of working fluid available to do work, resulting in lower power output.

This modified model aims to compare the relationship between the diameter of the displacer piston and the power output of the Stirling engine. By varying the diameter of the displacer piston, we can analyze how it affects the performance of the engine. This comparison helps in understanding the influence of displacer piston size on the engine's power generation capability, and overall effectiveness. Through this analysis, insights can be gained to optimize the design and operation of Stirling engines for improved performance.

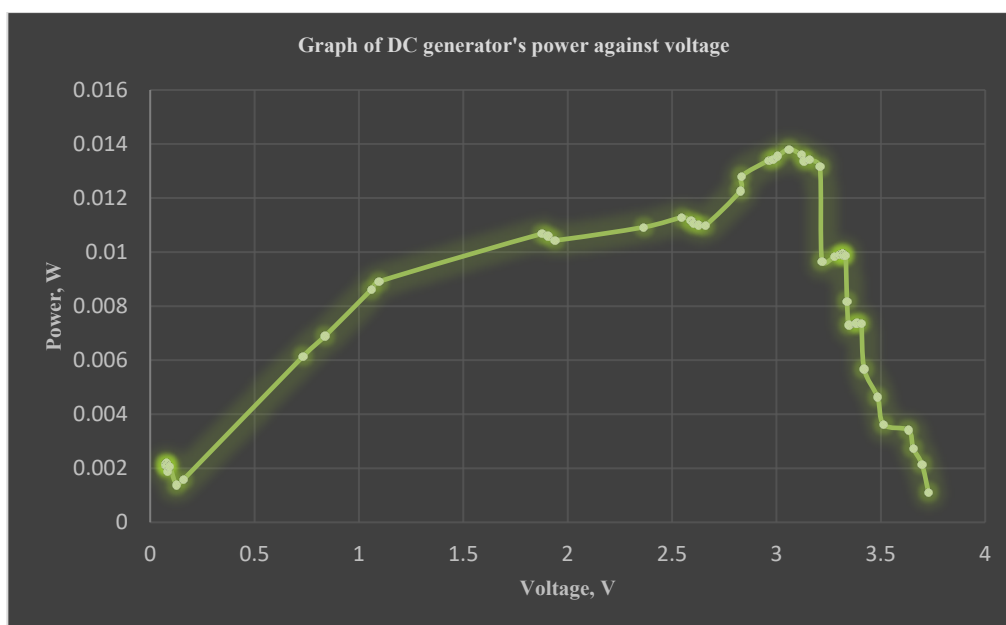


Figure 4.9: Graph of DC generator's power against voltage

4.3.4 Titanium Displacer with Diameter of 39mm (100° phase angle)

Figure 4.10 below shows the current-voltage graph of a Stirling engine system utilizing titanium material for the displacer piston, with the phase angle between the flywheels set at 100°, deviating from the previous models where it was set at 90°. Analysis of the graph reveals that the maximum current flow reaches approximately 0.038A when the variable resistor is at its lowest resistance. Similar to the previous models, an increase in the resistance of the variable resistor leads to a decrease in the current flow within the system. Conversely, there is an increasing trend in the voltage drop across the variable resistor. The peak voltage drop across the variable resistor reaches around 9V when the variable resistor is adjusted to its highest resistance, corresponding to the lowest current flow within the system, approximately 0.0009A.

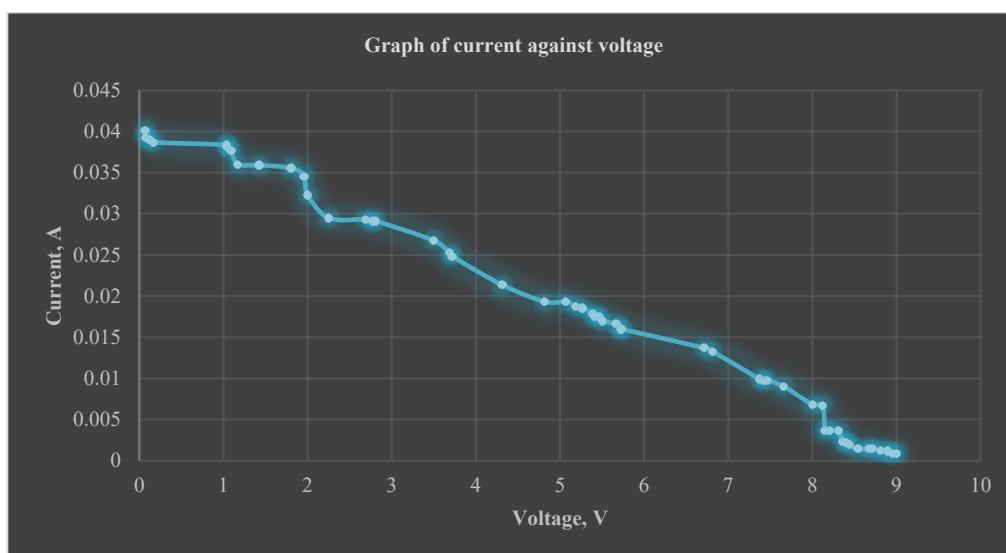


Figure 4.10: Graph of current against voltage

Figure 4.11 illustrates the relationship between the power generated by the DC generator and the voltage drop across the variable resistor within the Stirling engine system. This particular system uses a 39mm diameter titanium displacer piston paired with a flywheel featuring a 100° offset. Analysis of the graph indicates that the DC generator achieves its highest power output, reaching approximately 0.1W. This represents a notable advancement compared to previous models. The significant improvement underscores the critical role played by the phase angle of the flywheel within the Stirling engine. Adjusting this phase angle can substantially impact the output power of the engine, as demonstrated by the observed increase in power generation. In order to facilitate the DC generator in operating at its pinnacle of performance, namely generating an approximate output power of 0.1W, it is important to sustain the rotational speed of the Stirling engine within the specified range of 500 - 600rpm

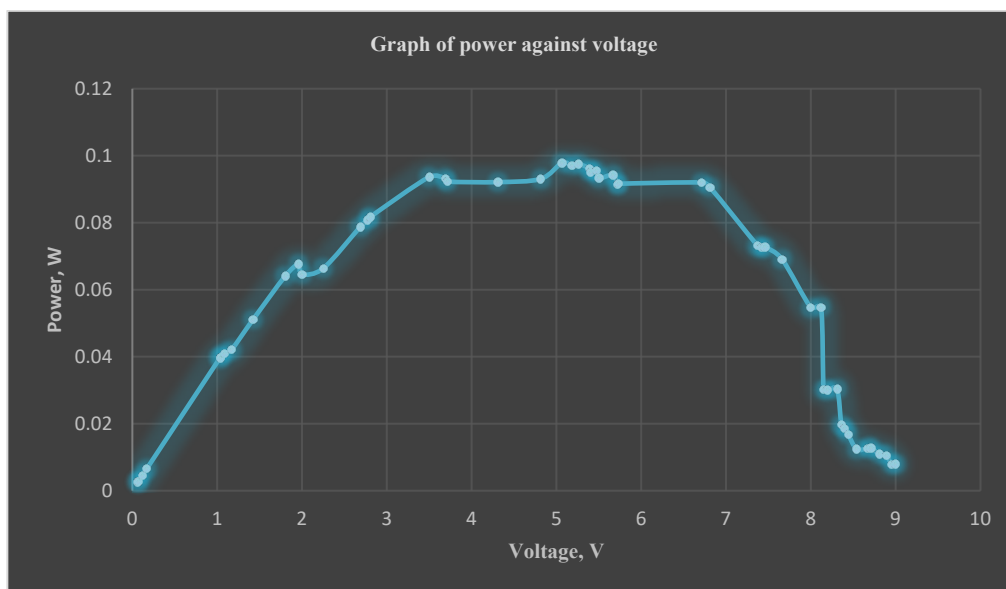


Figure 4.11: Graph of DC generator's power against voltage

4.4 Highest Achievable Output Power

Figure 4.12 provides a comprehensive comparison of the output power of various models of Stirling engines in relation to the output voltage. Each line on the graph represents a different Stirling engine configuration, showcasing the impact of different parameters on performance.

The blue line corresponds to a Stirling engine utilizing an aluminum displacer with a diameter of 39mm, coupled with a phase angle of 90° between the flywheels. This configuration serves as a reference point for comparison. The red solid line depicts the output power of a Stirling engine equipped with a titanium displacer of the same diameter (39mm) and phase angle (90°) as the blue model. The use of titanium, known for its lightweight and high strength, may result in improved performance compared to aluminum. Meanwhile, the green solid line represents another variation, featuring a titanium displacer with a slightly smaller diameter of 35mm while maintaining the same phase angle (90°). This configuration aims to explore the impact of displacer size on output power. Lastly, the purple solid line illustrates the output power of a Stirling engine employing a titanium displacer with the same diameter (39mm) as the red model but with a larger phase angle of 100° between the flywheels. This adjustment in phase angle seeks to assess its effect on engine performance.

Upon analysis of the graph, it can be observed that the Stirling engine utilizing the 39mm diameter titanium displacer with a phase angle of 100° demonstrates the highest output power among all configurations. This suggests that both the material composition and the phase angle between the flywheels have significant influences on the engine's performance. The findings from this comparison can inform future design considerations and optimizations aimed at maximizing Stirling engine efficiency and output power.

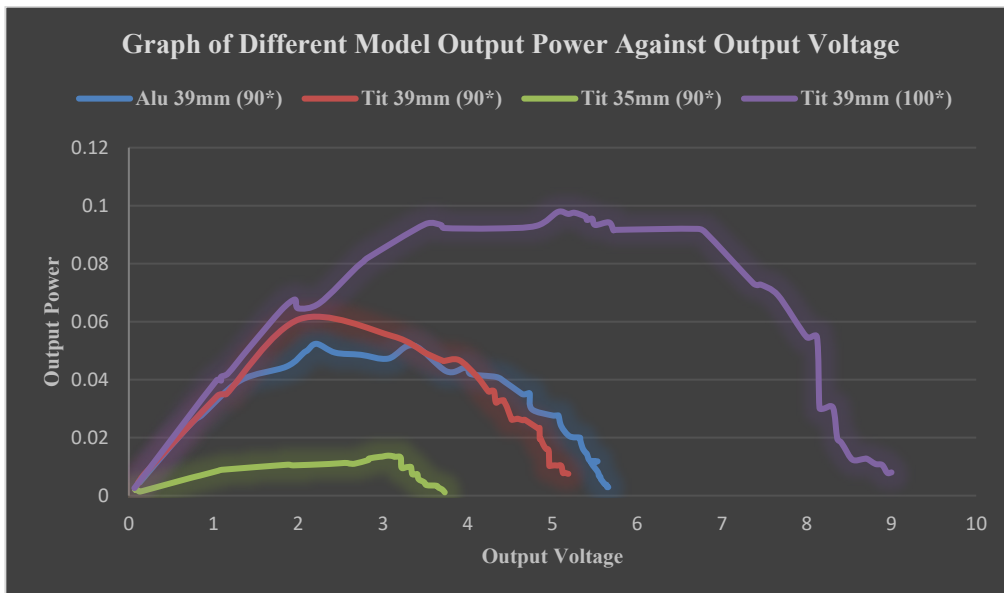


Figure 4.12: Highest Achievable Output Power of Different Model Stirling Engine

4.5 Charging Circuit Design

Figure 4.13 displays the upper side of the charging circuit board, showcasing the integration of essential components soldered onto the donut board. This assembly is meticulously crafted to minimize size, ensuring the prototype remains as compact as possible. Figure 4.14 shows the picture of the charging process of an 18650 battery. The presence of a red light indicates that the charging process is currently in progress.

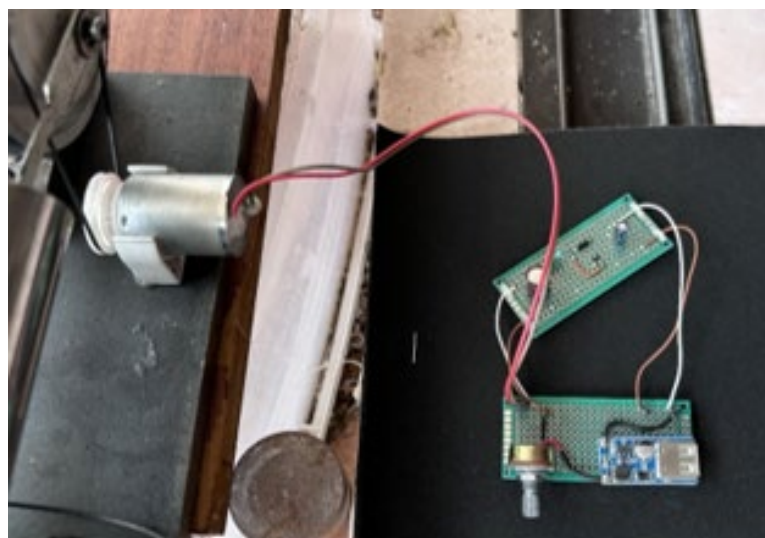


Figure 4.13: Charging circuit board

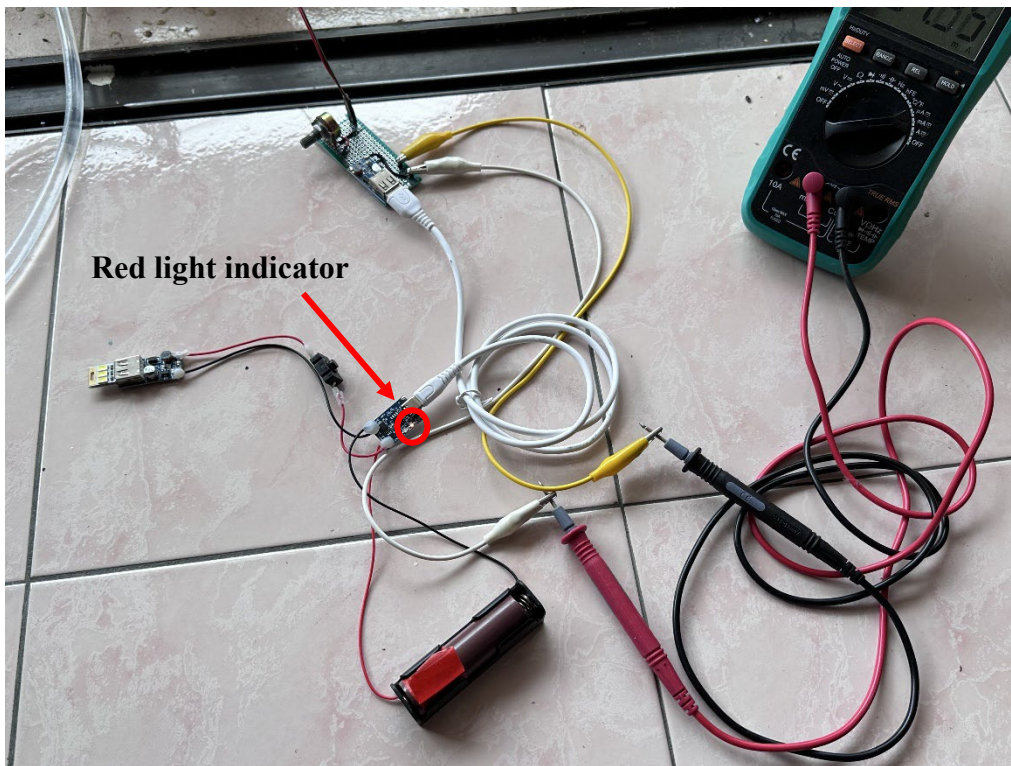


Figure 4.14: System charging indications

4.6 Summary

In this chapter, a detailed analysis of various Stirling engine configurations and their performance characteristics is presented. The aim is to examine the relationship between the output power and key parameters such as the material of the displacer, the diameter of the displacer, and the phase angle between the flywheel. Through the above graphical representations, the impact of these factors on Stirling engine performance is explained, offering valuable insights for design optimization. Specifically, comparisons are made between Stirling engines utilizing aluminum and titanium displacers of different diameters and phase angles between flywheels. The findings reveal that configurations featuring titanium displacers tend to exhibit higher output power, particularly when combined with larger diameter, and larger phase angles between flywheels. Lastly, these results highlight the importance of material selection and phase angle adjustment in maximizing Stirling engine efficiency.

CHAPTER 5

CONCLUSIONS AND RECOMMENDATIONS

5.1 Conclusions

In this proposed project, a Stirling engine has been constructed, utilizing materials provided by UTAR's mechanical lab. Subsequently, this Stirling engine served as the focal point for investigating methods to assess its performance as a prime mover for electricity generation. Additionally, it was utilized as a platform to explore strategies aimed at enhancing its efficiency and overall performance.

The comparison conducted in Chapter 4 explains the role of design parameters in influencing output power, revealing significant differences across various configurations. The excellent performance demonstrated by the Stirling engine equipped with a large diameter titanium displacer and a 100° phase angle. This finding emphasizes the importance of optimization in achieving heightened power output. Such insights are instrumental in advancing Stirling engine technology, guiding future research and development endeavors geared towards maximizing efficiency and performance.

In conclusion, the completion of this project contributes to a deeper understanding of Stirling engine dynamics, laying the groundwork for transformative advancements in sustainable energy solutions.

5.2 Problems Encountered

Throughout the development process of the Stirling engine, several problems that obstructed progress were encountered. One of the primary challenges was the limited understanding of the complex workings and fundamental principles underlying Stirling engine operation. This lack of familiarity with Stirling engine dynamics posed a significant barrier to achieving the start-up of the Stirling engine. Moreover, one critical issue encountered revolved around the phase angle between the flywheel of the Stirling engine. The phase angle of the flywheel plays a crucial role in determining the timing and synchronization of various mechanical movements within the Stirling engine. However, the initial attempts to configure the phase angle were met with difficulty, leading to inconsistencies in engine performance.

Besides that, the material selection for the displacer piston is also important due to the harsh thermal conditions it encounters during operation. It is important to choose a material that can withstand high temperatures without undergoing significant degradation. Initially, the displacer piston was made using tin, which needed superglue to bond the tin pieces together into a cylindrical form. Unfortunately, superglue is not designed to withstand the high temperatures experienced within the engine. Consequently, the displacer piston required frequent rebuilding. After identifying the problem, a spot welder machine was introduced instead of using super glue. Spot welding involves joining steel sheets together by applying heat and pressure to create a strong bond. By using spot welding instead of superglue, the issue of frequent displacer piston failures due to adhesive problems was effectively resolved.

Lastly, the scale of the constructed Stirling engine is not sufficiently large, resulting in a relatively low power output. The size of the Stirling engine plays a crucial role in determining its power-generating capacity. A larger engine typically has a greater capacity to produce power.

5.3 Recommendations for Future Enhancement

This study on the evaluation of the performance of the Stirling engine produced the desired outcome and achieved the objectives of the proposed project. However, there is further work and recommendations that can be undertaken to improve the entire generation system in the future to provide and produce higher output power. The following are the suggestions that can be implemented in the project.

Firstly, the scale of the Stirling engine. In future iterations, increasing the scale of the Stirling engine could be a focus area for improvement. This might involve redesigning components to accommodate larger dimensions, optimizing heat transfer mechanisms, and ensuring structural integrity at larger scales.

Secondly, efficiency optimization. Focus on improving the efficiency of the Stirling engine by enhancing heat transfer mechanisms, reducing frictional losses, and optimizing the gas cycle. This could involve exploring advanced heat exchanger designs, reducing internal leakage, and refining the engine's operating parameters.

REFERENCES

- Abuelyamen, A. and Ben-Mansour, R., 2018. Energy efficiency comparison of Stirling engine types (α , β , and γ) using detailed CFD modeling. Available at: <https://doi.org/10.1016/j.ijthermalsci.2018.06.026> [Accessed: 6 September 2023].
- Ahmadi, M.H. et al., 2013. Application of the multi-objective optimization method for designing a powered Stirling heat engine: Design with maximized power, thermal efficiency and minimized pressure loss. Available at: <http://dx.doi.org/10.1016/j.renene.2013.05.005> [Accessed: 14 September 2023].
- Alfarawi, S., Al-Dadah, R. and Mahmoud, S., 2016. Enhanced thermodynamic modelling of a gamma-type Stirling engine. *Applied Thermal Engineering*, 106, pp.1380–1390.
- Alfarawi, S., AL-Dadah, R. and Mahmoud, S., 2016. Influence of phase angle and dead volume on gamma-type Stirling engine power using CFD simulation. *Energy Conversion and Management*, 124, pp.130–140.
- Anon, *How do Stirling engines work? - Explain that Stuff* [Online]. Available at: <https://www.explainthatstuff.com/how-stirling-engines-work.html> [Accessed: 1 August 2023a].
- Anon, *Stirling engine: What is it and how it works? - Electrical e-Library.com* [Online]. Available at: <https://www.electricalibrary.com/en/2020/06/16/stirling-engine-what-is-it-and-how-it-works/> [Accessed: 25 April 2024b].
- Backhaus, S. and Swift, G.W., 1999. A thermoacoustic Stirling heat engine. *Nature* 1999 399:6734, 399(6734), pp.335–338. Available at: <https://www.nature.com/articles/20624> [Accessed: 19 October 2023].
- Beltr An-Chacon, R. et al., 2015. Design and analysis of a dead volume control for a solar Stirling engine with induction generator. Available at: <http://dx.doi.org/10.1016/j.energy.2015.09.046> [Accessed: 18 October 2023].
- Elrod, 1974. The fluidyne heat engine: how to build one -- how it works. Conference report.
- Kadri, Y. and Hadj Abdallah, H., 2016. Performance evaluation of a stand-alone solar dish Stirling system for power generation suitable for off-grid rural electrification. *Energy Conversion and Management*, 129, pp.140–156.
- Kongtragool, B. and Wongwises, S., 2006. Thermodynamic analysis of a Stirling engine including dead volumes of hot space, cold space and regenerator. *Renewable Energy*, 31(3), pp.345–359.
- Li, Y.H. et al., 2013. Combustion characteristics in a small-scale reactor with catalyst segmentation and cavities. *Proceedings of the Combustion Institute*, 34(2), pp.2253–2259.
- Li, Z., Tang, D., Du, J. and Li, T., 2011. Study on the radiation flux and temperature distributions of the concentrator–receiver system in a solar dish/Stirling power facility. *Applied Thermal Engineering*, 31(10), pp.1780–1789.

- Podesser, E., 1999. ELECTRICITY PRODUCTION IN RURAL VILLAGES WITH A BIOMASS STIRLING ENGINE. *Renewable Energy*, 16, pp.1049–1052.
- Senft, J.R., 2002. Optimum Stirling engine geometry. *International Journal of Energy Research*, 26(12), pp.1087–1101. Available at: <https://onlinelibrary.wiley.com/doi/full/10.1002/er.838> [Accessed: 6 September 2023].
- Senft, J.R. (James R.), 1993. Ringbom Stirling engines. , p.189.
- Shufat, S.A. et al., 2019. Exploration of a Stirling engine and generator combination for air and helium media. *Applied Thermal Engineering*, 150, pp.738–749.
- Singh, U.R. and Kumar, A., 2018. Review on solar Stirling engine: Development and performance. *Thermal Science and Engineering Progress*, 8, pp.244–256.
- Timoumi, Y., Tlili, I. and Nasrallah, S. Ben, 2008. Performance optimization of Stirling engines. *Renewable Energy*, 33, pp.2134–2144. Available at: www.elsevier.com/locate/renene [Accessed: 8 September 2023].
- Wu, C.Y. et al., 2021. The application of an innovative integrated Swiss-roll-combustor/Stirling-hot-end component on an unpressurized Stirling engine. *Energy Conversion and Management*, 249, p.114831.
- Zilanll, G.A. and Eray, A., 2017. Feasibility study of dish/stirling power systems in Turkey. *AIP Conference Proceedings*, 1850(1), p.45. Available at: [/aip/acp/article/1850/1/160029/616891/Feasibility-study-of-dish-stirling-power-systems](https://aip.acp/article/1850/1/160029/616891/Feasibility-study-of-dish-stirling-power-systems) [Accessed: 26 October 2023].